© 2022. Published by The Company of Biologists Ltd | Development (2022) 149, dev199625. doi:10.1242/dev.199625

RESEARCH ARTICLE

Msl3 promotes germline stem cell differentiation in female *Drosophila*

Alicia McCarthy[1], Kahini Sarkar[1], Elliot T. Martin[1], Maitreyi Upadhyay[1,2,*], Seoyeon Jang[3], Nathan D. Williams[3,4,‡], Paolo E. Forni[1], Michael Buszczak[3] and Prashanth Rangan[1,§]

ABSTRACT

Gamete formation from germline stem cells (GSCs) is essential for sexual reproduction. However, the regulation of GSC differentiation is incompletely understood. Set2, which deposits H3K36me3 modifications, is required for GSC differentiation during *Drosophila* oogenesis. We discovered that the H3K36me3 reader Male-specific lethal 3 (Msl3) and histone acetyltransferase complex Ada2a-containing (ATAC) cooperate with Set2 to regulate GSC differentiation in female *Drosophila*. Msl3, acting independently of the rest of the male-specific lethal complex, promotes transcription of genes, including a germline-enriched *ribosomal protein S19* paralog *RpS19b*. *RpS19b* upregulation is required for translation of RNA-binding Fox protein 1 (Rbfox1), a known meiotic cell cycle entry factor. Thus, Msl3 regulates GSC differentiation by modulating translation of a key factor that promotes transition to an oocyte fate.

KEY WORDS: Differentiation, Meiosis, Msl3, RpS19, Set2 and Rbfox1

INTRODUCTION

Germ cells give rise to gametes, a fundamental requirement for sexual reproduction. The production of gametes is tightly controlled to ensure a constant supply throughout the reproductive life of an organism (Cinalli et al., 2008; Kimble, 2011; Lehmann, 2012; Spradling et al., 1997). Germline stem cells (GSCs) divide mitotically to both self-renew and generate differentiating daughters that can enter meiosis (Kimble, 2011; Lehmann, 2012; Spradling et al., 2011). Loss of differentiation and meiotic entry results in infertility (Hughes et al., 2018; Lesch and Page, 2012; Soh et al., 2015).

GSC differentiation is well characterized during *Drosophila* oogenesis (Ables, 2015; Collins et al., 2014). *Drosophila* ovaries are composed of individual egg-producing units called ovarioles. A structure called the germarium lies at the tip of each ovariole and houses GSCs, which are marked by round organelles called spectrosomes (Eliazer and Buszczak, 2011; Morris and Spradling, 2011; Morrison and Spradling, 2008; Spradling et al., 2011, 2001, 2008) (Fig. 1A). GSCs both self-renew and differentiate into cystoblasts (CBs), which divide and undergo incomplete cytokinesis to give rise to two-, four-, eight- and 16-cell cysts, which are marked by branched structures called fusomes (Chen and McKearin, 2003a,b; Xie, 2013).

Early germ cell differentiation is controlled by both intrinsic and extrinsic factors (Flora et al., 2017; Spradling et al., 2011). The somatic niche of the germarium provides Decapentaplegic (DPP) signaling that leads to phosphorylation of Mothers against DPP (pMad) in GSCs, and transcriptional repression of the differentiation factor *bag of marbles* (*bam*) (Chen and McKearin, 2003a,b; Kai and Spradling, 2003). After GSC division, the CB is displaced from the niche, allowing for Bam expression (Chen and McKearin, 2003a,b). Bam is sufficient to promote the transition from CB to a differentiated eight-cell cyst (McKearin and Ohlstein, 1995; McKearin and Spradling, 1990).

In the eight-cell cyst, expression of cytoplasmic isoforms of RNA-binding Fox protein 1 (Rbfox1) leads to translational downregulation of self-renewal factors to promote expression of Bruno (Bru) (Carreira-Rosario et al., 2016; Tastan et al., 2010). Bru, in turn, translationally represses mitotic factors, which promote cyst divisions, and regulates entry into a meiotic cell cycle (Parisi et al., 2001; Sugimura and Lilly, 2006; Wang and Lin, 2007). Multiple cells in the cysts initiate meiosis, but only the oocyte will commit to meiosis; the other 15 cells acquire a nurse cell fate in the 16-cell cyst stage (Carpenter and Sandler, 1974; Huynh and St Johnston, 2004; Mach and Lehmann, 1997; Navarro et al., 2001; Theurkauf et al., 1993). The oocyte and the 15 nurse cells are encapsulated by somatic cells to form a developing egg chamber and eventually an egg (Fig. 1A1). Although Rbfox1 expression in the germline is essential for entry into a meiotic cell cycle and oocyte specification, how it is induced is unclear (Carreira-Rosario et al., 2016).

Another hallmark of meiosis, apart from a specialized cell cycle, is homologous chromosome recombination. This process is regulated by the formation of the synaptonemal complex (SC) (Ables, 2015; Hughes et al., 2018). The SC starts to assemble on homologs in two cells with four ring canals, and to a lesser degree in the other 14 cells of the cyst, and it then becomes restricted to the future oocyte (Page and Hawley, 2001; Von Stetina and Orr-Weaver, 2011) (Fig. 1A). Although proper homologous recombination is not required for differentiation, it is required for fertility (Collins et al., 2014; Handel and Schimenti, 2010). How transcription of SC components is activated during meiosis is not well understood.

GSC differentiation during *Drosophila* oogenesis requires the histone methyltransferase SET domain containing 2 (Set2), which confers histone H3 lysine 36 trimethylation (H3K36me3) (Larschan et al., 2007; Mukai et al., 2015; Stabell et al., 2007). H3K36me3 typically marks transcriptionally active genes (Bannister and Kouzarides, 2011; Dong and Weng, 2013; Keogh et al., 2005). How H3K36me3 regulates GSC differentiation is not clear.

[1]Department of Biological Sciences/RNA Institute, University at Albany SUNY, Albany, NY 12202, USA. [2]Department of Stem Cell and Regenerative Biology, Harvard University, Cambridge, MA 02138, USA. [3]Department of Molecular Biology, University of Texas Southwestern Medical Center, Dallas, TX 75390, USA. [4]Department of Cell Biology, Yale University School of Medicine, New Haven, CT 06520, USA.
*Present address: Department of Stem Cell and Regenerative Biology, Harvard University, Cambridge, MA 02138, USA. ‡Present address: Department of Cell Biology, Yale University School of Medicine, New Haven, CT 06520, USA.

§Author for correspondence (prangan@albany.edu)

A.M., 0000-0003-0060-3592; P.R., 0000-0002-1452-8119

Received 29 March 2021; Accepted 19 November 2021

Development (2022) 149, dev199625. doi:10.1242/dev.199625

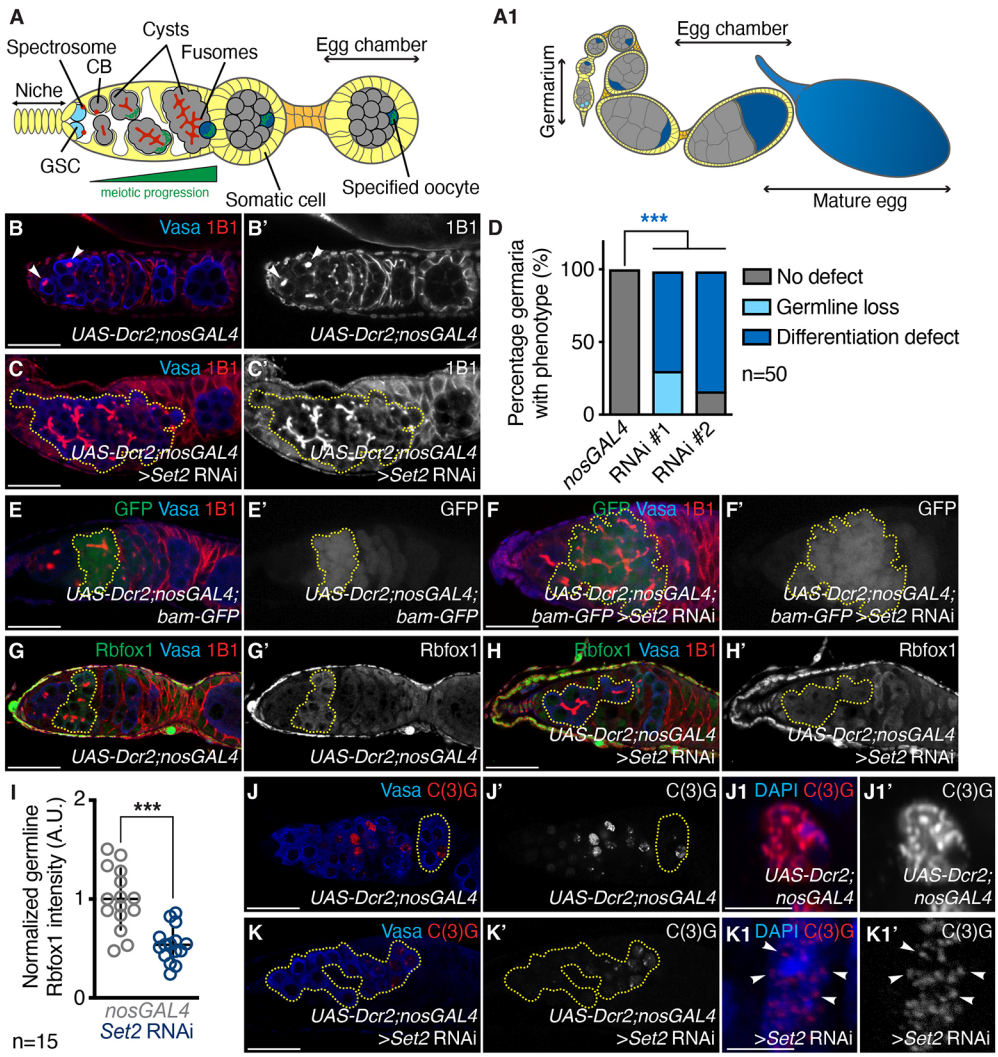

Fig. 1. Set2 is required in the germline for differentiation during oogenesis. (A) Schematic of a *Drosophila* germarium where germ cells (gray, and light and dark blue) are surrounded by somatic cells (yellow). Germ cells differentiate and specify an oocyte (green/blue). (A1) A schematic of a *Drosophila* ovariole showing egg chambers that house a maturing oocyte (blue) connected by somatic cells (orange). (B,B′) Control and (C,C′) germline-depleted *Set2* (RNAi line #1) germaria stained for Vasa (blue) and 1B1 (red) show that *Set2* germline depletion results in differentiation defects such as accumulation of irregular cysts with >16 cells (yellow dashed outline), accumulation of 16-cell cysts close to the niche and loss of GSCs (white arrowheads in control). The 1B1 channel is shown in B′ and C′. (D) Quantitation of B-C′. Data are percentage of germaria. Fisher's exact test; ***P<0.001. (E,E′) Control and (F,F′) germline-depleted *Set2* germaria both carrying a *bam-GFP* transgene stained for GFP (green), Vasa (blue) and 1B1 (red) show that *Set2* germline depletion results in irregular GFP-positive cysts compared with control (yellow dashed outline) (90% in *Set2* RNAi compared with 4% in *nosGAL4*; P<2.2E-16, n=50, Fisher's exact test). GFP channel is shown in E′ and F′. (G,G′) Control and (H,H′) germline-depleted *Set2* germaria stained for Rbfox1 (green), Vasa (blue) and 1B1 (red) show that *Set2* germline depletion results in decreased levels of Rbfox1 in the germline compared with control (yellow dashed outline). Rbfox1 channel is shown in G′ and H′. (I) Quantitation of G-H′, Student t-test; ***P<0.001. (J-J1′) Control and (K-K1′) germline-depleted *Set2* germaria stained for Vasa (blue) and C(3)G (red) show that *Set2* germline depletion results in aberrant C(3)G staining compared with control (yellow dashed outline) (100% in *Set2* RNAi compared with 2% in *nosGAL4*; P<2.2E-16, n=50) and improper assembly of the synaptonemal complex (white arrowheads). Statistical analysis, Fisher's exact test. Data are mean±95% CI. C(3)G channel is shown in J′, J1′, K′ and K1′. Scale bars: 20 µm for B-C′,E-H′,J,J′,K,K′; 2 µm for J1,J1′,K1,K1′.

Interestingly, in male *Drosophila*, H3K36me3 facilitates recognition of the X chromosome by the Male-Specific Lethal (Msl) complex, which leads to hyper-transcription of the male X and gene dose compensation with females, which have two X chromosomes (Bell et al., 2008; Conrad et al., 2012b; Larschan et al., 2007). Within the MSL complex, the chromodomain (CD) of Msl3 reads H3K36me3 marks and the histone acetyl transferase (HAT) Males absent on the first (MOF) deposits acetylation of histone H4 lysine 16 (H4K16ac) (Bone et al., 1994; Conrad et al., 2012a; Gu et al., 2000; Hilfiker et al., 1997; Larschan et al., 2007). Female flies do not assemble the MSL complex because key components, including Msl2, are not expressed at sufficient levels (Bashaw and Baker, 1997; Kelley et al., 1997; UCHIDA et al., 1981). However, whether individual MSL proteins in *Drosophila* regulate gene expression beyond their role in dose compensation is not known.

Here, we find that Set2, Msl3 and a HAT complex, Ada2a-containing (ATAC), promote GSC differentiation. We discovered that Msl3 is expressed in the early stages of oogenesis, where it promotes the HAT-mediated transcription of several members of the SC, as well as a germline-specific paralog of eukaryotic *Ribosomal protein S19* (*eRpS19*/*RpS19*). Expression of RpS19b (S19b) helps increase overall levels of RpS19, which is then required for translation of *Rbfox1* and thus promotes GSC differentiation into an oocyte.

Development (2022) 149, dev199625. doi:10.1242/dev.199625

RESULTS

Set2 is required in the germline for proper differentiation

To determine how *Set2* promotes oogenesis in *Drosophila*, we stained control and *Set2* depleted fly gonads with antibodies against Vasa, a germline marker, and 1B1, a marker of somatic cell membranes, spectrosomes and fusomes. Compared with controls, *Set2*-depleted gonads displayed a loss of spectrosome containing GSCs, an accumulation of fusome-containing cysts and a loss of proper egg chamber formation (Fig. 1B-D; Fig. S1A-B′). The *Set2*-depleted germaria accumulated eight- and 16-cell cysts, as well cysts that were multinucleated up to 64 cells (n=30). The egg chambers that do form contain undifferentiated and differentiating cells marked by spectrosomes and fusomes that fail to develop further (100% in *Set2* RNAi compared with 0% in *nosGAL4*; P<2.2E-16, n=50), resulting in females that are infertile. Additionally, *Set2*-depleted germ cells had significantly reduced H3K36me3 levels compared with the control, consistent with previous reports (Mukai et al., 2015) (Fig. S1C-E).

The accumulation of cyst-like structures upon germline depletion of *Set2* could be due to GSCs that divide but fail to undergo cytokinesis, resulting in GSC cysts or in differentiating cysts that cannot progress further in development (Carreira-Rosario et al., 2016; Mathieu and Huynh, 2017; Sanchez et al., 2016). To discern between these two types of cyst, we stained for pMad, a marker of GSCs. In addition, we crossed a *bam* transcriptional reporter, *bam-GFP*, into the Set2 RNAi background and independently assayed for Bam protein (Chen and McKearin, 2003b). We found that *Set2* RNAi germaria accumulated differentiating cysts, which transcribed and then translated Bam, and were pMad negative (Fig. 1E-F′; Fig. S1F-I′). Thus, *Set2* is required in the germline downstream of *bam* to promote the differentiation of Bam-expressing cysts into egg chambers.

Although germline depletion of *Set2* leads to both loss of GSCs and accumulation of cysts, here we focus on the cyst accumulation phenotype. Loss of *Set2* results in cysts that do not properly express the oocyte-specific protein Orb (Mukai et al., 2015), but loss of Orb does not phenocopy loss of *Set2*, suggesting that Orb downregulation is a consequence of the differentiation defect (Barr et al., 2019; Christerson and McKearin, 1994; Huynh and St Johnston, 2000). Similar to loss of *Set2*, loss of Rbfox1 results in the accumulation of Bam-expressing cysts that do not differentiate into proper egg chambers (Carreira-Rosario et al., 2016; Tastan et al., 2010). To test whether *Set2* regulates Rbfox1 and Bru expression, we stained separately for Rbfox1 and Bru along with Vasa and 1B1 in control and germline *Set2*-depleted ovaries. Although control germaria express Rbfox1 robustly in eight-cell cysts, *Set2*-depleted germ cells exhibited a significantly lower level of Rbfox1, while somatic levels were unchanged (Fig. 1G-I). Furthermore, Bru levels were reduced and enrichment in the oocyte was ablated in *Set2* RNAi germaria compared with controls (Fig. S1J-L). Thus, *Set2* is required after Bam expression to promote proper differentiation via Rbfox1 expression.

As germline depletion of *Set2* results in reduced levels of Rbfox1 and Bru, we hypothesized that *Set2*-depleted cysts do not properly enter meiosis or specify an oocyte. We stained control and *Set2*-depleted germaria with antibodies against a SC member, Crossover suppressor on 3 of Gowen [C(3)G], and Vasa (Anderson et al., 2005; Page and Hawley, 2001). The control had several C(3)G-positive germ cells in 16-cell cysts but only the most posterior germ cell in the egg chamber was marked with C(3)G. In *Set2* germline-depleted germaria, the majority of cells displayed perturbed C(3)G expression; an irregular number of cells were C(3)G positive and C(3)G appeared fragmented (Fig. 1J-K1′). To determine whether the oocyte is properly specified, we stained for the oocyte determinant Egalitarian (Egl), as well as for Vasa and 1B1 (Carpenter, 1994; Huynh and St Johnston, 2000; Mach and Lehmann, 1997). Although control 16-cell cysts had a single Egl-positive cell, *Set2* germline-depleted germaria showed diffuse staining of Egl without enrichment in a single cell (Fig. S1M-N′). Thus, the H3K36me3-depositing enzyme Set2 is required for proper differentiation and oocyte specification.

Msl3 acts downstream of Set2 to promote proper differentiation independently of the MSL complex

To identify readers of H3K36me3 that activate transcription downstream of Set2, we screened 18 known Chromodomain (CD)-containing proteins, which recognize lysine methylation marks, for loss-of-function phenotypes that phenocopied Set2 (Allis and Jenuwein, 2016; McCarthy et al., 2018; Navarro-Costa et al., 2016). Unexpectedly, of the 18 CD-containing proteins that we examined by RNAi knockdown, only Msl3 displayed a cyst accumulation phenotype (see Table S1). Msl3 is a reader of H3K36me3 mark that promotes dose compensation in the soma in male flies, where it acts within the MSL complex (see Lucchesi and Kuroda, 2015), but whether Msl3 has a role in the female *Drosophila* germline has not been examined.

As a first test, we investigated Msl3 expression in ovaries. We analyzed *msl3* transcript levels at different stages of oogenesis, using RNA-seq libraries that we enriched for GSCs, CBs, cysts and adult whole ovaries, as previously described (McKearin and Ohlstein, 1995; Xie and Spradling, 1998; Zhang et al., 2014). We found that *msl3* mRNA is expressed during oogenesis, consistent with what was reported on FlyBase (The Modencode Consortium et al., 2010) (Fig. S2A). We also examined ovaries from a fly line expressing GFP-tagged Msl3 under endogenous control (Strukov et al., 2011), by staining for GFP and 1B1. We found that Msl3-GFP was expressed in the germline in single cells marked by spectrosomes and early cysts marked by fusomes (Fig. 2A-A′; Fig. S2B). Thus, unlike Msl2 (Bashaw and Baker, 1997; Parisi et al., 2001), Msl3 is expressed at appreciable levels during early stages of oogenesis at both the RNA and protein level.

To verify our RNAi knockdown experiments indicating a role in oogenesis, we examined validated *msl3* mutants (Bachiller and Sánchez, 1989; Sural et al., 2008; UCHIDA et al., 1981). As background mutations in *msl3* mutant stocks have been described to cause synthetic lethality (Erickson, 2016; Gladstein et al., 2010), we analyzed three independent alleles from different genetic backgrounds. We created trans-allelic combinations of independent *msl3* mutations to eliminate potential deleterious effects of homozygous background mutations; these combinations lead to cyst accumulation monitored by accumulation of fusome-positive cells, germline loss monitored by absence of Vasa-positive cells, and a reduction in formation of proper egg chambers (Fig. 2B-D; Fig. S2C-D′). Furthermore, as our screen indicated depletion of *msl3* in the germline alone, using RNAi resulted in the accumulation of cysts, which phenocopied *msl3* mutants (Fig. 2D, Fig. S2E-F′). The cysts that accumulate upon *msl3* germline depletion expressed *bam* but were pMad negative and failed to properly express Rbfox1 or Bru, phenocopying *Set2* germline depletion (Fig. 2E-I; Fig. S2G-M). In addition, these cysts failed to specify an oocyte, as monitored by Egl, and showed reduced expression of the synaptonemal protein C(3)G (Fig. 2J-K1′; Fig. S2N-O′). Last, expression of *msl3* in the germline of *msl3* mutant females was sufficient to rescue the differentiation defect (Fig. 2D,L,M). Taken together, we conclude

Development (2022) 149, dev199625. doi:10.1242/dev.199625

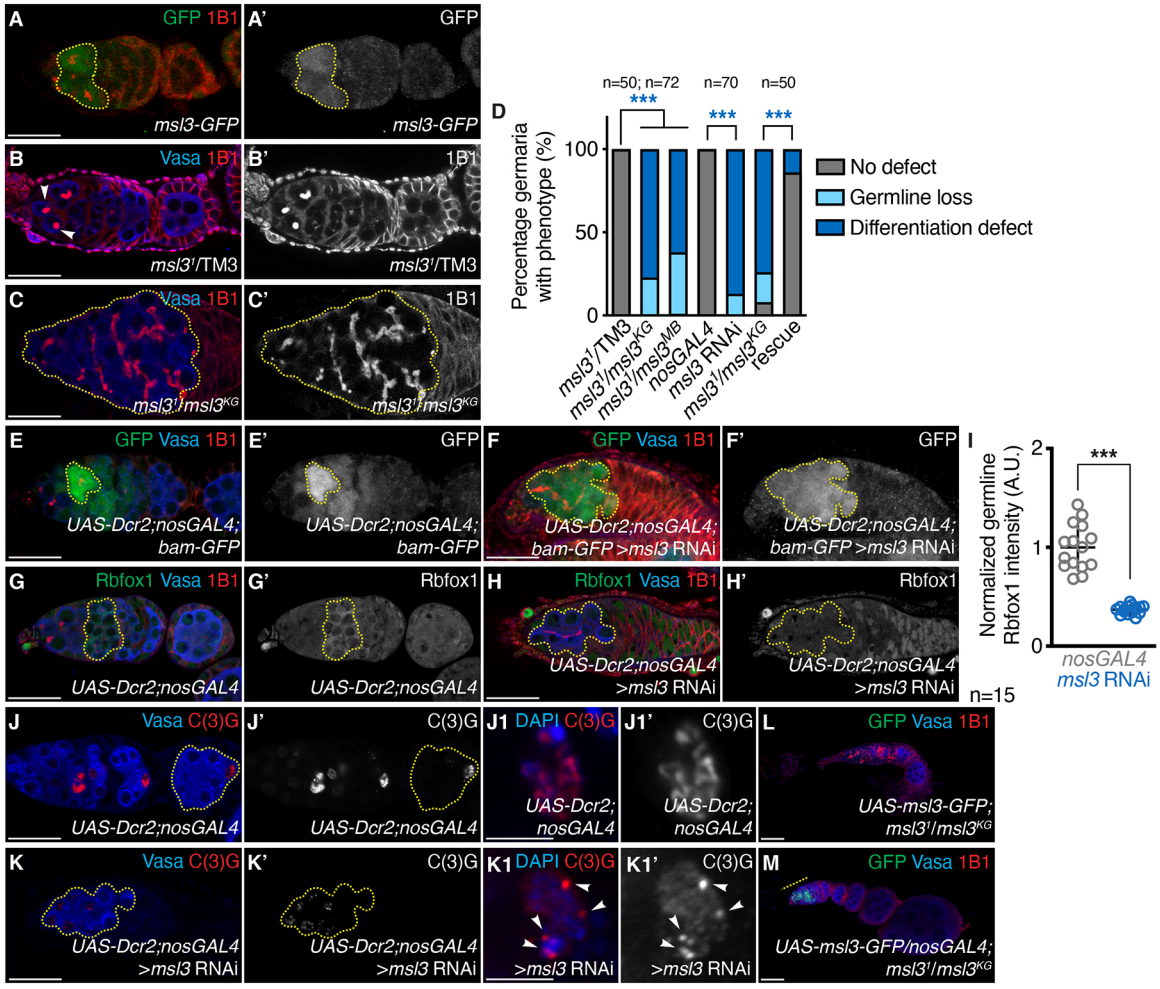

Fig. 2. Msl3 is required in the germline for differentiation. (A,A′) *msl3-GFP* germarium stained for GFP (green) and 1B1 (red). GFP expression is enriched in single cells and early cysts, showing that Msl3 is expressed in the mitotic and early meiotic stages of oogenesis. GFP channel is shown in A′. (B,B′) Heterozygous control and (C,C′) trans-allelic *msl3* mutant germaria stained for Vasa (blue) and 1B1 (red) show that *msl3* mutants have differentiation defects, such as accumulation of irregular cysts with >16 cells (yellow dashed outline), accumulation of 16-cell cysts close to the niche and loss of GSCs. Arrowheads in B indicate spectrosomes. 1B1 channel is shown in B′ and C′. (D) Quantitation of B-C′. Data are percentage of germaria. Fisher's exact test; ***P<0.001. (E,E′) Control and (F,F′) germline-depleted *msl3* germaria both carrying a *bam-GFP* transgene stained for GFP (green), Vasa (blue) and 1B1 (red) show that *msl3* germline depletion results in irregular GFP-positive cysts compared with control (yellow dashed outline) (96% in *msl3* RNAi compared with 0% in *nosGAL4*; P<2.2E-16, n=50, Fisher's exact test). GFP channel is shown in E′ and F′. (G,G′) Control and (H,H′) germline-depleted *msl3* germaria stained for Rbfox1 (green), Vasa (blue) and 1B1 (red) show that *msl3* germline depletion results in decreased levels of Rbfox1 in the germline compared with control (yellow dashed outline). The Rbfox1 channel is shown in G′ and H′. (I) Quantitation of G-H′. Data are mean±95% CI. Student's t-test; ***P<0.001. (J,J′) Control and (K,K′) germline-depleted *msl3* germaria stained for Vasa (blue) and C(3)G (red) show that *msl3* germline depletion results in aberrant C(3)G staining compared with control (yellow dashed outline) (100% in *msl3* RNAi compared with 0% in *nosGAL4*; P<2.2E-16, n=50, Fisher's exact test) and improper assembly of the synaptonemal complex (white arrowheads in K1 and K1′). The C(3)G channel is shown in J′, J1′, K1 and K1′. (L) Control and (M) germline overexpression of *msl3* in *msl3* mutant germaria stained for GFP (green), Vasa (blue) and 1B1 (red) shows that *msl3* germline overexpression in *msl3* mutants results in reduced frequency of irregular cysts (yellow dashed line) (14% in *msl3* rescue compared with 74% in *msl3* mutant; P<2.2E-16, n=50) and germline loss (0% in *msl3* rescue compared with 18% in *msl3* mutant; P=0.0002, n=50). Scale bars: 20 µm for A-C′,E-H′,J-K′,L,M; 2 µm for J1,J1′,K1,K1′.

that Msl3 is required in the female germline to promote proper differentiation.

To determine whether the H3K36me3 writer Set2 and the H3K36me3 reader Msl3 act together to promote oogenesis, we generated flies heterozygous for *Set2* and *msl3*. Although the trans-heterozygous flies were viable, their germaria displayed severe germline loss compared with single heterozygous controls (Fig. S3A-C). Although loss of Msl3 did not affect H3K36me3 levels, loss of *Set2* attenuated Msl3 expression (Fig. S3D-H). Together, these data suggest that Set2 and Msl3 impinge upon the same developmental pathway(s), with Msl3 acting downstream of Set2 to promote proper differentiation.

This function of Msl3 during oogenesis is independent of its role in the MSL complex, as we found that *msl2*, *roX1* and *roX2* are barely expressed (<1 TPM), consistent with previous reports (Bashaw and Baker, 1997; Meller et al., 1997; Parisi et al., 2004). Additionally, validated *msl1*, *msl2* and *mle* mutants (Bachiller and Sánchez, 1989; Belote, 1983; UCHIDA et al., 1981) did not result in early oogenesis defects (Fig. S3I), nor did loss of germline MOF (Sun et al., 2015).

The ATAC complex acts with Set2 and Msl3 to promote proper differentiation

We asked whether the H3K36me3 reader Msl3 cooperates with another HAT-containing complex to regulate cyst differentiation.

Development (2022) 149, dev199625. doi:10.1242/dev.199625

Using an RNAi screen, we found that members of the Ada2a-containing (ATAC) complex phenocopy loss of *Set2* and *msl3* in the germline (McCarthy et al., 2018; Spedale et al., 2012; Suganuma et al., 2008) (Fig. 3A-C; Fig. S4A-H). The ATAC complex contains 13 proteins, some shared with other complexes, including Gcn5 (Spedale et al., 2012). Depletion of six members, four of which are specific to the ATAC complex, resulted in the accumulation of cysts and germline loss (Fig. S4A-H), Of these ATAC complex members, we chose to focus on Negative Cofactor 2β (NC2β), as its defect was highly penetrant but maintained sufficient germline for transcriptomic analysis.

Loss of NC2β in the germline led to GSC loss monitored by loss of spectrosome containing cells and accumulation of cysts-like structures that were marked by fusomes (Fig. 3A-C; Fig. S4A-B′). To determine whether the cysts that accumulate due to loss of *NC2β* phenocopy cysts that accumulate due to loss of *Set2* and *msl3*, we independently probed for GSC marker pMad and differentiation markers Bam, Rbfox1 and Bru. In addition, we also probed for meiotic marker C(3)G. We found that cysts that accumulate upon germline depletion of NC2β expressed Bam, did not contain pMad-positive cells or properly express Rbfox1 or Bru (Fig. 3D-H; Fig. S5A-G). In addition, loss of *NC2β* leads to meiotic defects and oocyte specification, as monitored by C(3)G localization and Egl, respectively (Fig. 3I-J1′; Fig. S5H-I′). These data suggest that the ATAC complex is required for proper differentiation, as well as oocyte specification that phenocopies loss of *Set2* and *msl3*.

As components of the ATAC complex phenocopy loss of the H3K36me3 writer *Set2* and the H3K36me3 reader *msl3*, we asked whether the ATAC complex acts downstream of H3K36me3 mark to promote proper meiosis. To test this, we stained for H3K36me3 in *NC2β* RNAi flies and found that H3K36me3 levels were unaltered, suggesting that ATAC complex acts downstream of *Set2* (Fig. S5J-L). In addition, we made use of a mutant of the active HAT in the ATAC complex, Atac2, as there were no *NC2β* mutants available. We generated flies heterozygous for both *Atac2* and *msl3*, and found that although trans-heterozygotes flies were viable, their germaria had severe defects compared with controls (Fig. S5M-O). Thus, the ATAC complex works downstream of Set2, and *Atac2* genetically interacts with *msl3*. Taken together, our data suggest that Set2, Msl3 and the ATAC complex impinge upon the same developmental pathway(s) to regulate differentiation in the *Drosophila* female germline.

Set2, Msl3 and NC2β promote transcription of the ribosomal protein paralog RpS19b

To determine how Set2, Msl3 and ATAC promote differentiation, we compared the transcriptomes of *Set2*, *msl3* and *NC2β* germline-depleted ovaries to a developmental control that accumulates cysts. To enrich for cysts, we induced *bam* expression under the control of a heat-shock (*hs*) promoter in the background of germaria depleted for *bam* (*bam* RNAi;*hs-bam*) (Ohlstein and McKearin, 1997; Zhang et al., 2014). We found 662 significantly downregulated and 65 significantly upregulated RNAs in *Set2*-depleted germaria compared with *bam* RNAi;*hs-bam* ovaries [fold change >|4|; False discovery rate (FDR)<0.05] (Fig. 4A). There were 283 significantly downregulated RNAs and 302 significantly upregulated RNAs in *msl3* RNAi compared with *bam* RNAi;*hs-bam* (Fig. 4A′). Last, there were 466 RNAs significantly downregulated and 277 upregulated in *NC2β* RNAi compared with the developmental control (Fig. 4A″). Set2 and ATAC are part of the generalized transcriptional machinery and are expected to regulate more genes than Msl3 alone. This is evident in the RNA-seq results, where we find more downregulated targets upon the loss of *Set2* (662 targets) and *NC2β* (466 targets) than loss of *msl3* (283 targets) (Fig. 4A-A″). Of those transcripts that were differentially expressed in *Set2*-, *msl3*- and *NC2β*-depleted germ cells compared with the *bam* RNAi;*hs-bam* control, there were 29 shared RNAs that were downregulated (Fig. 4B) and 11 shared RNAs that were upregulated (see Table S2). This small but significant overlap of targets suggests a specific subset of Msl3 targets are co-regulated by Set2 and ATAC.

Although Rbfox1 protein is not properly expressed upon loss of Set2, Msl3 and NC2β, *Rbfox1* mRNA was not among the shared downregulated RNAs (Fig. 4C). We verified that *Rbfox1* mRNA was present in the germline of *msl3*-depleted ovaries by *in situ* hybridization (Fig. S6A-B′). Thus, Set2, Msl3 and ATAC do not regulate *Rbfox1* mRNA levels to promote differentiation. In contrast, we found that several SC member genes were among the shared downregulated genes, including *orientation disruptor* (*ord*), *sisters unbound* (*sunn*) and *corona* (*cona*) (Hughes et al., 2018), but C(3)G was not among those genes (Fig. 4D,E; Fig. S6C,D). To validate the loss of SC components, we crossed an Ord-GFP line that is under endogenous control (Balicky et al., 2002) into *msl3* mutants and found that *msl3* mutant ovaries had both lower levels and an altered location of Ord-GFP compared with controls (Fig. S6E-F′). Although this change can be mediated by both RNA levels or protein stability, we found *ord* nascent mRNAs levels are also downregulated (see below). The shared downregulated targets also included 11 candidate genes (CGs) of unknown function, and the ribosomal protein paralog RpS19b (S19b), but not RpS19a (S19a) (Fig. 4B,F; Fig. S6G-J′).

We hypothesized that Msl3 and Msl3-regulated mRNAs would be expressed at the same stages, from GSCs until the cyst stages. To test this hypothesis, we analyzed mRNA levels of the 29 targets in RNA-seq libraries enriched for either GSCs, CBs, cysts or unenriched wild-type ovaries. Indeed, transcript levels overlapped with Msl3 expression and then dropped off (Fig. 4G). Last, to determine whether SC genes and *RpS19b* were affected at the level of transcription, we measured nascent mRNA (pre-mRNA) levels, using qRT-PCR as a proxy for transcription. We found that, upon depletion of *msl3*, nascent mRNA levels of SC genes and RpS19b are significantly lower (Fig. 4H). Taken together, these data suggest that Set2, Msl3 and ATAC regulate transcription of SC components and *RpS19b*, but not *Rbfox1*, during differentiation. Although loss of SC components leads to loss of recombination, it does not cause a differentiation defect (Collins et al., 2014). Proper cyst differentiation is mediated by Rbfox1 (Carreira-Rosario et al., 2016; Tastan et al., 2010). Altogether, this suggests that a target of Set2, Msl, and ATAC regulates not *Rbfox1* mRNA levels but another aspect of expression of the gene – potentially its translation to promote differentiation.

RpS19b is a germline-enriched ribosomal protein required for Rbfox1 translation

RpS19b is a ribosomal protein and is one of two RpS19 paralogs in *Drosophila.* Given that loss of Set2, Msl3 and NC2β decreased Rbfox1 protein levels without affecting *Rbfox1* mRNA levels, we hypothesized that the reduced RpS19b expression we observed in these mutants resulted in the decreased translation of *Rbfox1* mRNA. If RpS19b is required for Rbfox1 translation, then the RpS19b protein should be present when Rbfox1 protein expression occurs. We examined lines expressing RpS19b-GFP and RpS19a-HA from under endogenous control. RpS19b-GFP was germline enriched, whereas RpS19a-HA was expressed in both the germline

Development (2022) 149, dev199625. doi:10.1242/dev.199625

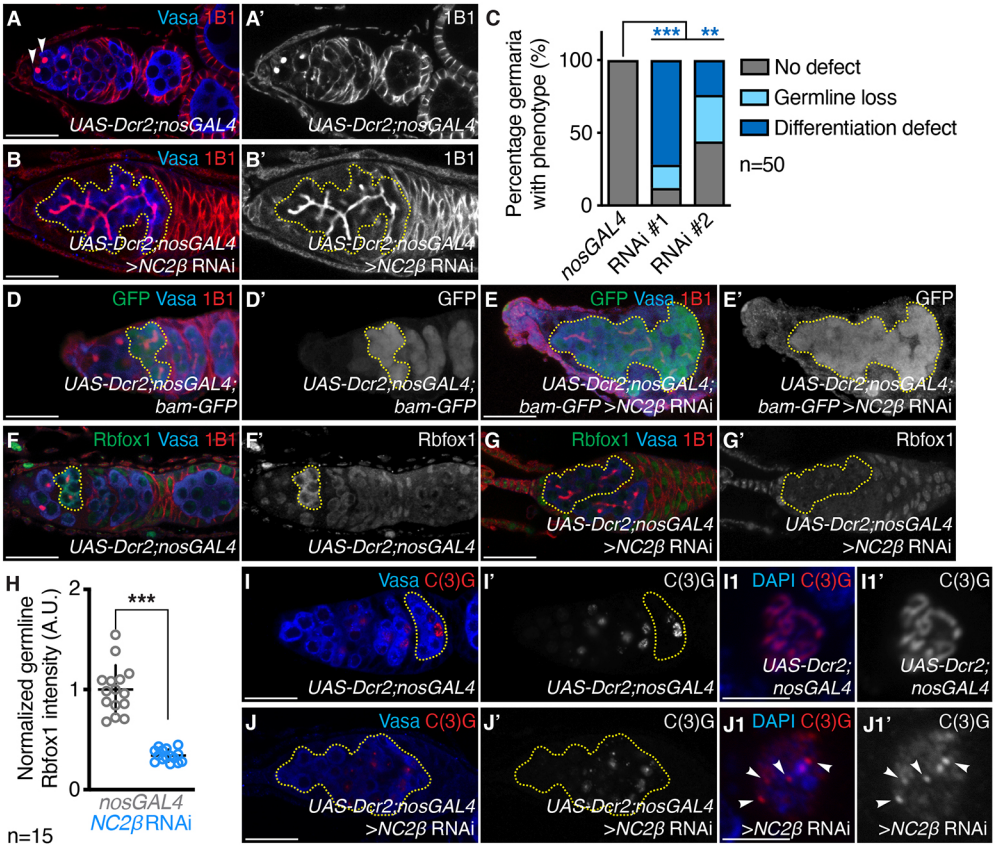

Fig. 3. The ATAC component NC2β is required in the germline for differentiation. (A,A′) Control and (B,B′) germline-depleted *NC2β* germaria stained for Vasa (blue) and 1B1 (red) show that *NC2β* germline depletion results in differentiation defects such as accumulation of irregular cysts with >16 cells (yellow dashed outline), accumulation of 16-cell cysts close to the niche and loss of GSCs. 1B1 channel is shown in A′ and B′. (C) Quantitation of A-B′. Data are percentage of germaria. Fisher's exact; ***P*<0.01; ****P*<0.001. (D,D′) Control and (E,E′) germline-depleted *NC2β* germaria both carrying a *bam-GFP* transgene stained for GFP (green), Vasa (blue) and 1B1 (red) show that *NC2β* germline depletion results in accumulation of irregular GFP-positive cysts compared with control (yellow dashed outline) (64% in *NC2β* RNAi compared with 0% in *nosGAL4*; *P*=2.5E-13, *n*=50, Fisher's exact test). GFP channel is shown in D′ and E′. (F, F′) Control and (G,G′) germline-depleted *NC2β* germaria stained for Rbfox1 (green), Vasa (blue) and 1B1 (red) show that *NC2β* germline depletion results in decreased levels of Rbfox1 in the germline compared with control (yellow dashed outline). Rbfox1 channel is shown in F′ and G′. (H) Quantitation of F-G′. Data are mean±95% CI. Student's *t*-test; ****P*<0.001. (I,I′,I1,I1′) Control and (J,J′,J1,J1′) germline-depleted *NC2β* germaria stained for Vasa (blue) and C(3)G (red) show that *NC2β* germline depletion results in aberrant C(3)G staining compared with control (yellow dashed outline and white arrowheads) (75% in *NC2β* RNAi compared with 0% in *nosGAL4*; *P*<2.2E-16, *n*=50) and improper assembly of the synaptonemal complex (white arrows). C(3)G channel is shown in I′, I1′, J′ and J1′. Scale bars: 20 µm for A-B′,D-G′,I,I′,J,J′; 2 µm for I1,I1′,J1,J1′.

and soma of the gonad (Fig. 5A-A1; Fig. S7A,B). In the germline, RpS19b-GFP was expressed at high levels in single cells and gradually decreased in cyst stages, which overlapped with the protein expression of Msl3 and Rbfox1 (Fig. 5B).

If RpS19b acts downstream of Msl3 to promote the translation of *Rbfox1* mRNA, then loss of RpS19b should result in reduced Rbfox1 protein levels and a germline phenotype that phenocopies that of *msl3*. We used RNAi to specifically deplete *RpS19b* but not *RpS19a* in the germline (Fig. S7C-F′) and found that *RpS19b*-depleted germaria accumulated *bam*-positive cysts that lack Rbfox1 protein (Fig. 5C-H; Fig. S7G-H′). To test whether *RpS19b* is one of the main targets of *msl3*, we asked whether the addition of *RpS19b* could rescue the differentiation defect of *msl3* mutants. Adding one copy of *RpS19b-GFP* in *msl3* mutant flies rescued the early cyst defect, including Rbfox1 expression, and led to egg chamber formation (Fig. 5I-M). Overexpression of *RpS19b* could also rescue the differentiation defect upon germline depletion of *msl3*, leading to egg chamber formation (Fig. 5N,O). Thus, our data suggest that Msl3 promotes the expression of RpS19b and thus *Rbfox1* translation and proper differentiation.

Our model predicts that the Msl3-mediated transcription of the SC members *ord*, *sunn* and *cona* is independent of Rbfox1 protein expression. To test this model, we examined the localization of the SC component C(3)G in *msl3* mutants that express RpS19b (Anderson et al., 2005; Page and Hawley, 2001). C(3)G was not a co-regulated target and thus allowed us to visualize SC defects. We found that while *msl3* mutants with restored RpS19b expression make egg chambers, C(3)G does not properly localize to the oocyte nucleus in egg chambers and the females are infertile (Fig. 5P-Q′). Thus, RpS19b is not involved in Msl3-mediated transcriptional regulation of SC members to promote recombination during meiosis.

RpS19 levels, not paralog specificity, are critical for proper differentiation

To validate the role of RpS19b in oogenesis, we generated a CRISPR null mutant of the gene ($RpS19b^{CRISPR}$). This null is viable but unexpectedly did not display any oogenesis defects in contrast to *RpS19b* RNAi (Fig. S7I-K). Studies in organisms, including zebrafish, have reported transcriptional compensation in mutants, but not upon depletion by RNAi (El-Brolosy et al., 2019). To

Development (2022) 149, dev199625. doi:10.1242/dev.199625

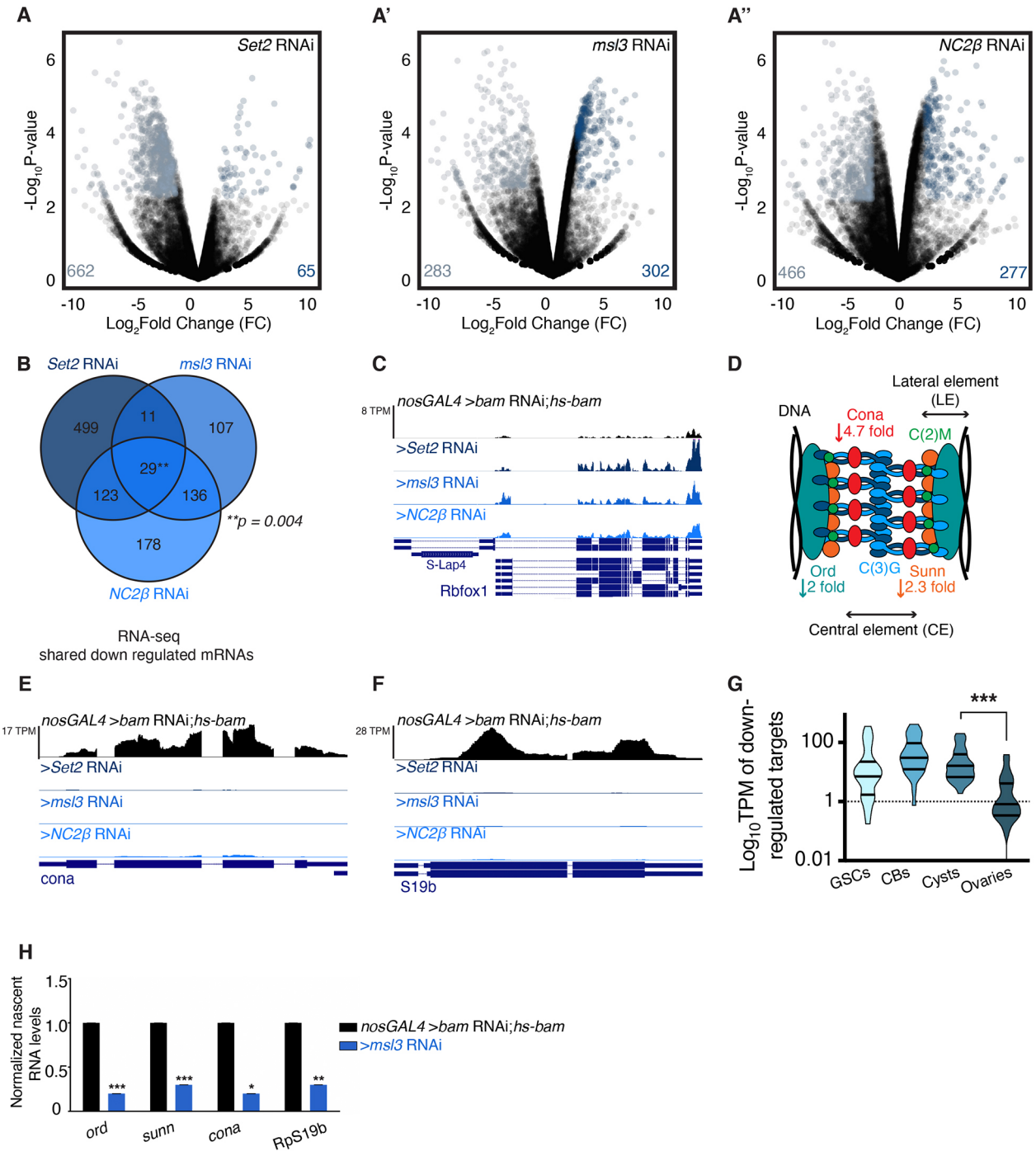

Fig. 4. Set2, Msl3 and the ATAC complex regulate mRNA levels of recombination machinery components, but not *Rbfox1*. (A-A″) Volcano plots of –Log_{10}P-value versus Log_2Fold Change (FC) of (A) *Set2*, (A′) *msl3* and (A″) *NC2β* germline-depleted ovaries compared with *bam* RNAi;*hs-bam*. Genes with fourfold or higher changes were considered significant (FDR=0.05). (B) Venn diagram of downregulated genes from RNA-seq of *Set2*, *msl3* and *NC2β* germline-depleted ovaries compared with *bam* RNAi;*hs-bam*. (C) RNA-seq track showing that *Rbfox1* is not reduced upon germline depletion of *Set2*, *msl3* and *NC2β*. (D) A structural model of the SC consisting of proteins such as Ord (teal), Sunn (orange) and C(2)M (green) assemble along DNA. Downward arrows denote fold downregulation of SC components in depleted ovaries. (E) RNA-seq track showing that *cona* is reduced upon germline depletion of *Set2*, *msl3* and *NC2β*. (F) RNA-seq track showing that *RpS19b* is reduced upon germline depletion of *Set2*, *msl3* and *NC2β*. (G) Violin plot of mRNA levels of the 29 shared downregulated targets in ovaries enriched for GSCs, GSC daughters, cysts and whole ovaries, showing that the shared targets are expressed up to cyst stages, that then attenuate in whole ovaries (one-way ANOVA; ***P<0.001). (H) qRT-PCR measuring levels of nascent mRNA levels of *ord*, *sunn*, *cona* and *RpS19b* upon depletion of *msl3* showing reduction compared with developmental control. Student's *t*-test; *P<0.05, **P<0.01, ***P<0.001.

determine whether the $RpS19b^{CRISPR}$ mutants display transcriptional changes, we performed RNA-seq of CB-enriched ovaries from control and $RpS19b^{CRISPR}$ flies, both with a *bam*-depleted background to enrich for the undifferentiated stages in which *RpS19b* is primarily expressed. We found that loss of *RpS19b* resulted in 79 downregulated genes and 934 upregulated genes, with ninefold downregulation of *RpS19b* but no increase in *RpS19a* RNA levels (Fig. S7L). As RpS19a mRNA levels were not altered,

Development (2022) 149, dev199625. doi:10.1242/dev.199625

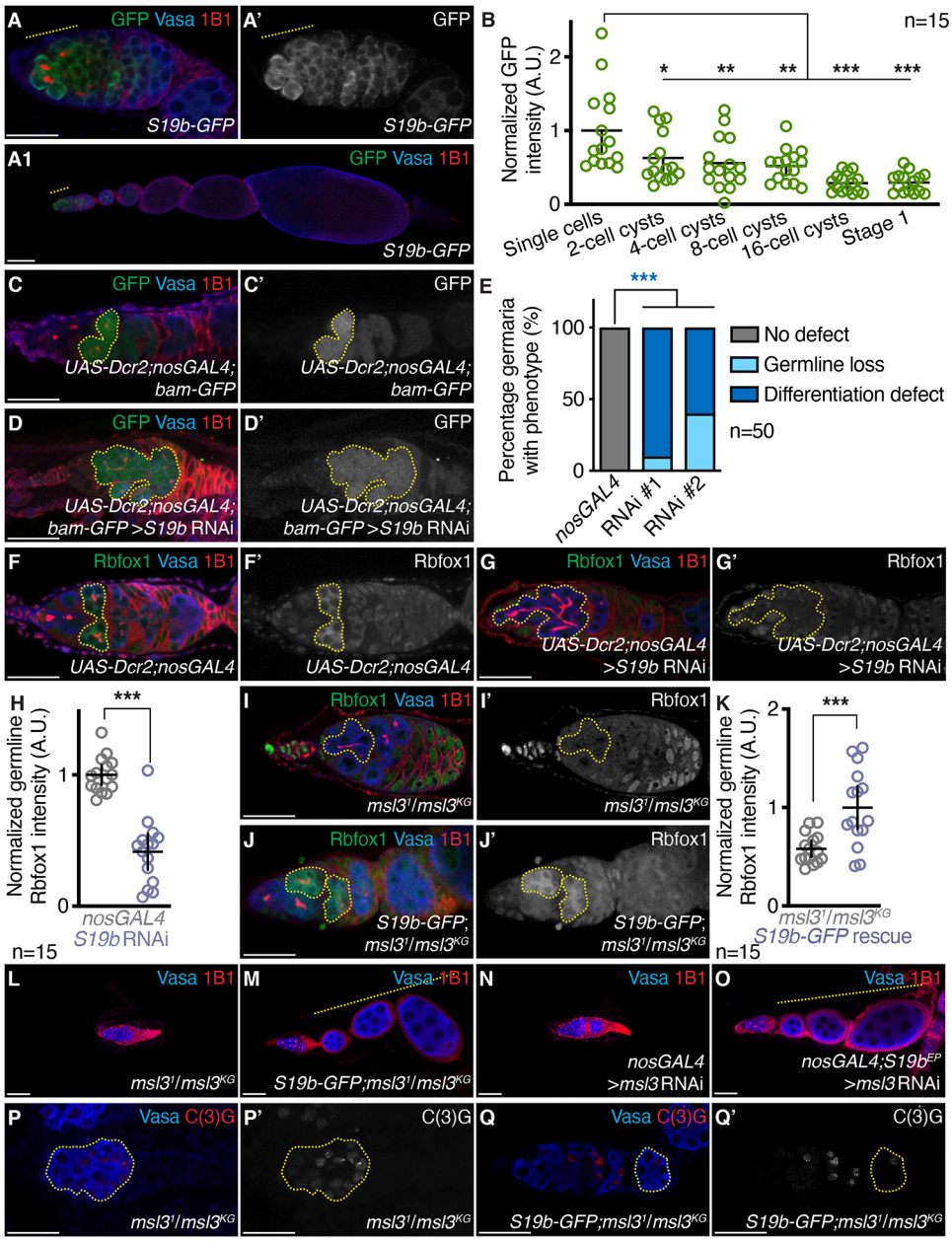

Fig. 5. RpS19b, a germline-enriched paralog, is expressed in the mitotic and early meiotic stages, and is required for Rbfox1 expression. (A,A′) *RpS19b-GFP* germarium and (A1) ovariole stained for GFP (green), Vasa (blue) and 1B1 (red). GFP is visible up to the cyst stages and then attenuated. GFP channel is shown in A′. (B) Quantitation of A,A′. Data are mean±95% CI. One-way ANOVA; **P*<0.05, ***P*<0.01 and ****P*<0.001. (C,C′) Control and (D,D′) germline-depleted *RpS19b* germaria both carrying a *bam-GFP* transgene stained for GFP (green), Vasa (blue) and 1B1 (red) show cysts with more than 16 cells that are GFP positive in *RpS19b* germline depletion compared with control (yellow dashed line). GFP channel is shown in C′ and D′. (E) Quantitation of C-D′. Data are percent germaria. Fisher's exact test on differentiation defect; ****P*<0.001. (F,F′) Control and (G,G′) germline-depleted *RpS19b* germaria stained for Rbfox1 (green), Vasa (blue) and 1B1 (red) show that *RpS19b* germline depletion results in decreased levels of Rbfox1 compared with control (yellow dashed outline). Rbfox1 channel is shown in F′ and G′. (H) Quantitation of F-G′. Data are mean±95% CI. Student's *t*-test; ****P*<0.001. (I,I′) Control and (J,J′) *RpS19b-GFP* rescue germaria stained for Rbfox1 (green), Vasa (blue) and 1B1 (red) show that addition of *RpS19b-GFP* to *msl3* mutants results in increased levels of Rbfox1 expression compared with control. Rbfox1 channel is shown in I′ and J′. (K) Quantitation in of I-J′. Data are mean±95% CI. Student's *t*-test; ****P*<0.001. (L) Control and (M) *RpS19b-GFP* rescue ovarioles stained for Vasa (blue) and 1B1 (red) show that addition of *RpS19b-GFP* to *msl3* mutants results in an increased frequency of spectrosomes and cysts (92% in *RpS19b-GFP* rescue compared with 4% in $msl3^{1}/msl3^{KG}$; *P*<2.2E-16, *n*=50), and of subsequent egg chambers compared with control (yellow dashed line) (98% in *RpS19b-GFP* rescue compared with 16% in $msl3^{1}/msl3^{KG}$; *P*<2.2E-16, *n*=50, Fisher's exact test). (N) Control and (O) $RpS19b^{EP}$ rescue ovarioles stained for Vasa (blue) and 1B1 (red) show that expression of $RpS19b^{EP}$ in *msl3* germline-depleted ovaries results in an increased frequency of spectrosomes and cysts (90% in $RpS19b^{EP}$ rescue compared with 0% in *msl3* RNAi; *P*<2.2E-16, *n*=50), and of subsequent egg chambers compared with control (yellow dashed line) (100% in $RpS19b^{EP}$ rescue compared with 4% in *msl3* RNAi; *P*<2.2E-16, *n*=50, Fisher's exact test). (P,P′) Control and (Q,Q′) *RpS19b-GFP* rescue germaria stained for Vasa (blue) and C(3)G (red) show that rescue and control germaria have aberrant C(3)G expression (yellow dashed outline) (96% in *RpS19b-GFP* rescue compared with 100% in $msl3^{1}/msl3^{KG}$; *P*=0.5, *n*=50). Addition of *RpS19b-GFP* does not rescue egg-laying defects (38 eggs/female in *RpS19b-GFP*, 32 eggs/female in $msl3^{1}$ heterozygote and 101 eggs/female in $msl3^{KG}$ heterozygotes compared with 0 eggs/female in $msl3^{KG}/msl3^{1}$ and rescue; *P*=0.02 for $msl3^{KG}/msl3^{1}$ and *P*=0.03 for rescue, *n*=4, Fisher's exact test). C(3)G channel is shown in P′ and Q′. Scale bars: 20 µm.

Development (2022) 149, dev199625. doi:10.1242/dev.199625

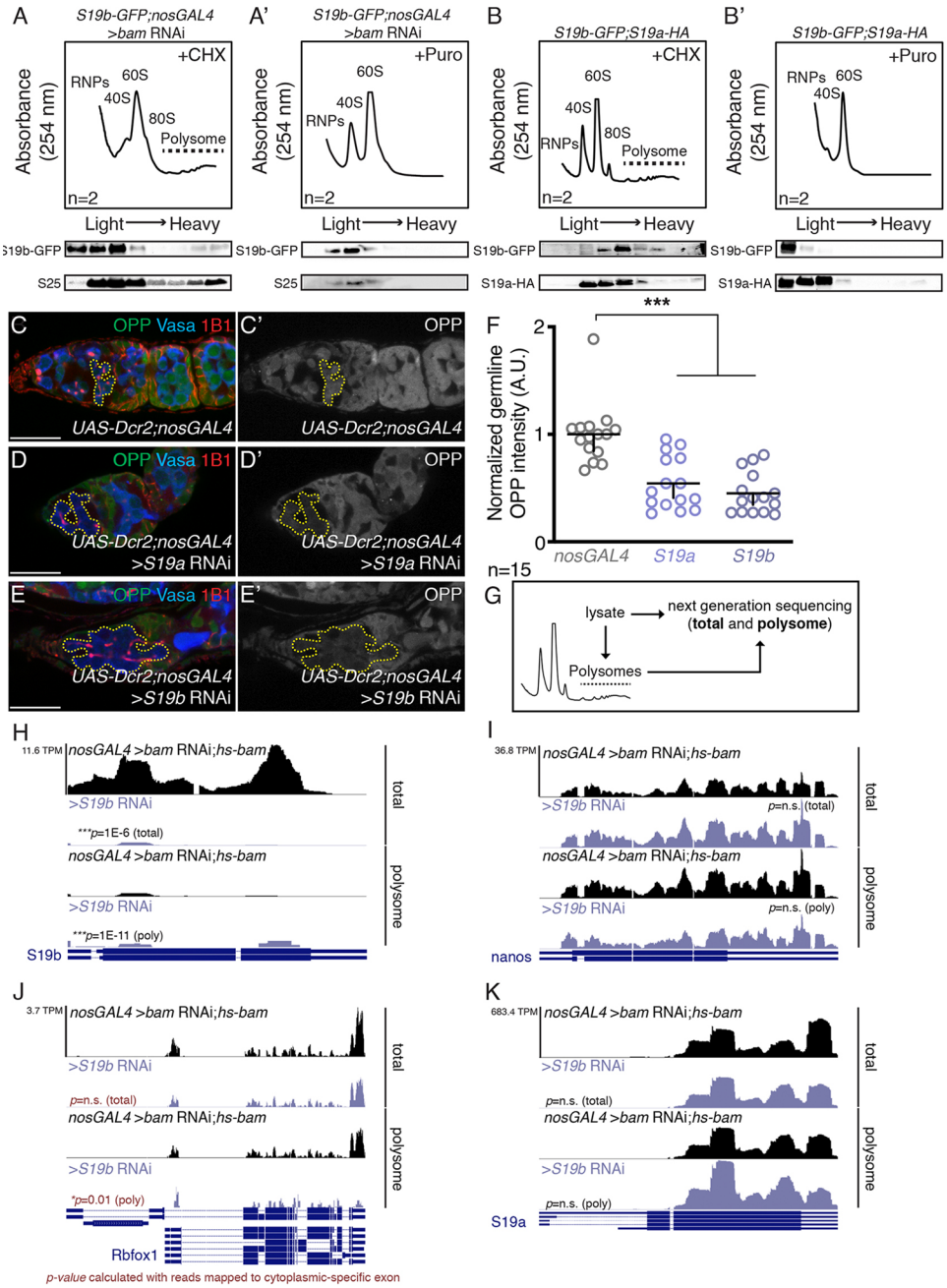

Fig. 6. RpS19 paralogs are incorporated into the ribosome and RpS19 levels affect translation, including translation of Rbfox1. (A,A′) Top: polysome profiles of *RpS19b-GFP;nosGAL4>bam* RNAi ovaries treated with cycloheximide (CHX, A) or puromycin (A′). Bottom: western blot of (A) cycloheximide (CHX) or (A′) puromycin. Blots were stained for GFP (top) and RpS25 (bottom), showing RpS19b and RpS25 bands in heavy fractions in CHX-treated samples that are absent in puromycin-treated samples. (B,B′) Top: polysome profiles of *RpS19b-GFP;RpS19a-HA* whole ovaries treated with cycloheximide (CHX, B) or puromycin (B′). Bottom: western blot of cycloheximide (B, CHX) or puromycin (B′). Blots were stained for HA (top) and GFP (bottom), showing RpS19a and RpS19b bands in heavy fractions in CHX-treated samples that are absent in puromycin-treated samples. (C,C′) Control and (D,D′) germline-depleted *RpS19a* and (E-E′) *RpS19b* germaria pulsed with OPP (green) and stained for Vasa (blue) and 1B1 (red) show that *RpS19a* and *RpS19b* germline depletion results in decreased OPP compared with control. The OPP channel is shown in C′, D′ and E′. (F) Quantitation of C-E′. Data are mean±95% CI. One-way ANOVA; ***P<0.001. (G) A schematic of the experimental approach to polysome-seq: RNA is extracted (total) with polysome fractionation (polysome) followed by sequencing. (H) RNA-seq track of total (top) and polysome (bottom) showing that *RpS19b* is reduced upon germline depletion of *RpS19b* (purple) compared with control (black) (total: Log_2FC=-4.1, P=1E-6, n=2 and polysome: Log_2FC=-4.5; P=1E-11, n=2). Student's t-test; ***P<0.001. (I) RNA-seq track of total (top) and polysome (bottom) showing that *nanos* and amount of germline is not reduced upon germline depletion of *RpS19b* (purple) compared with control (black) (total: Log_2FC=0.4; P=0.4, n=2 and polysome: Log_2FC=0.3; P=*0.7*, n=2). Student's t-test; n.s. indicates P>0.5. (J) RNA-seq track of total (top) and polysome (bottom) showing that cytoplasmic *Rbfox1* is reduced in polysome fractions upon germline depletion of *RpS19b* (purple) compared with control (black) (total: P=0.2, n=2; polysome: P=0.01, n=2). Student t-test; n.s. indicates P>0.5 and *P<0.05. (K) RNA-seq track of total (top) and polysome (bottom) showing that *RpS19a* is not reduced upon germline depletion of *RpS19b* (purple) compared with control (black) (total: Log_2FC=-0.4; P=0.4, n=2 and polysome: Log_2FC=-0.1; P=0.9, n=2). Student's t-test; n.s. indicates P>0.5. Scale bars: 20 µm.

Development (2022) 149, dev199625. doi:10.1242/dev.199625

we then asked whether *RpS19b* mutants have proper development because they have increased levels of RpS19a protein. Using a RpS19 antibody that detects both paralogs, we found that levels of RpS19 were not downregulated in $RpS19b^{CRISPR}$ mutant gonads compared with the control (Fig. S7M-P). Furthermore, germline depletion of *RpS19a* in $RpS19b^{CRISPR}$ mutants results in the complete loss of the germline, although there is no defect at all in homozygous $RpS19b^{CRISPR}$ mutants and only the accumulation of cysts upon *RpS19a* depletion alone (Fig. S7Q-R). In contrast, *RpS19b* depletion in $RpS19b^{CRISPR}$ mutants resulted in no defect (Fig. S7S-T). Thus, we conclude that full loss of RpS19b can be compensated for by increased levels of RpS19a in $RpS19b^{CRISPR}$ but not in *RpS19b* RNAi, via as yet unknown mechanisms.

These data suggest that what is required for Rbfox1 translation is a critical level of RpS19, which can be provided by either the RpS19a or S19b isoforms, or by a combination of both. To test this, we depleted *RpS19a* from the germline and found that the germaria accumulate *bam*-positive cysts that have significantly reduced levels of Rbfox1 (Fig. S8A-L′). Ectopic expression of RpS19a-HA in *msl3*-depleted ovaries that have reduced levels of RpS19b restored Rbfox1 protein expression and egg chamber formation (Fig. S8M-P). Consistent with our previous data showing that Rps19b cannot rescue expression of SC components in the *msl3* mutant, these females were also infertile and had perturbed C(3)G localization (Fig. S8Q-R). Furthermore, expression of human RpS19 in the germline of *msl3*-depleted germaria also was able to rescue the cyst accumulation phenotype, leading to the production of normal egg chambers (Fig. S8S-T1). Thus, our data taken together suggest that a proper dose of RpS19 is essential for the translation of Rbfox1 protein.

RpS19 promotes *Rbfox1* translation in the germline

We next examined the requirement for RpS19 in Rbfox1 translation. First, to determine whether RpS19a and S19b were incorporated into actively translating ribosomes, we performed polysome profiling followed by western blot analysis using wild-type ovaries and those enriched for undifferentiated germ cell cysts (*bam* RNAi). Although RpS19a-HA is present in polysome fractions in wild type ovaries, RpS19b-GFP appears to be preferentially enriched in polysomes from ovaries enriched for undifferentiated germ cells, consistent with its expression pattern early in oogenesis (Fig. 6A-B′). To test whether RpS19 paralogs affect translation in cysts, we pulsed gonads with a puromycin analog, O-propargyl-puromycin (OPP), that is incorporated into translated peptides and can be detected using Click-chemistry (Sanchez et al., 2016). We found that cysts that accumulate upon the loss of RpS19a and RpS19b have decreased translation compared with cysts of control ovaries (Fig. 6C-F). Thus, we find that RpS19a and S19b are present in the translating polysomes and are important for translation in cysts.

To directly test whether RpS19b is required for *Rbfox1* translation specifically, we then performed polysome-seq on germaria depleted of *RpS19b* compared with control germaria enriched for cysts using *bam RNAi*;*hs-bam* (Fig. 6G,H). Depletion of germline *RpS19b* did not significantly affect the translation of the germline-specific mRNA *nanos*, but there was a reduction in *Rbfox1* cytoplasmic isoform mRNA translation compared with the control (Fig. 6I-J). Additionally, depletion of *RpS19b* using RNAi, did not reduce the levels or translation efficiency of *RpS19a* (Fig. 6K). Taken together, our data suggest that there is an increased expression of RpS19 during early development that is required for translation of *Rbfox1* mRNA.

DISCUSSION

We have identified Set2, Msl3 and the ATAC complex as transcriptional regulators of differentiation and proper meiosis in *Drosophila*. We find that Set2, Msl3 and ATAC together regulate oogenesis downstream of the differentiation factor Bam, but upstream of the crucial differentiation factor Rbfox1. Although we find significant shared targets between Set2, Msl3 and NC2β that control differentiation, the total number of shared targets is small. One reason for this could also be the ability of Msl3 to read H4K20me1 marks (Kim et al., 2010), allowing it to affect a distinct set of targets than those marked by the H3K36me3 laid down by Set2. Similarly, Msl3 could recruit a different HAT from the one associated with NC2β, one that functions in the undifferentiated stages (McCarthy et al., 2018). Thus, we hypothesize that Set2, Msl3 and ATAC work in concert on a select subset of targets to regulate meiosis and oogenesis.

We find that recruitment by Msl3 of the basal transcriptional machinery, ATAC to the Set2-mediated H3K36me3 marks, would lead to enhanced transcription of a subset of genes that promote differentiation at the proper stage. We do not know what controls the expression of Msl3 itself during oogenesis. *msl3* mRNA is present as part of the maternal contribution deposited into the developing oocyte (Eichhorn et al., 2016; Hua et al., 2014) This suggests that *msl3* mRNA is also transcribed in the later stages of oogenesis and is likely post-transcriptionally regulated in the later stages. Although our data demonstrates that Msl3 expression is required for proper differentiation in female *Drosophila*, we do not think Msl3 expression is sufficient for differentiation, as overexpression of *msl3* does not lead to precocious differentiation (Fig. 2L,M).

We find that Set2, Msl3 and ATAC regulate oogenesis in two ways: (1) they transcriptionally upregulate members of the synaptonemal complex that are crucial for recombination; and (2) they promote transcription of the germline-enriched *RpS19* paralog *RpS19b*. The expression of RpS19b then controls the translation of *Rbfox1*, which is required for exit from the mitotic cell cycle and entry into the meiotic cell cycle (Fig. 7). Although several components of the synaptonemal complex, Cona, Ord and Sunn, are regulated at the

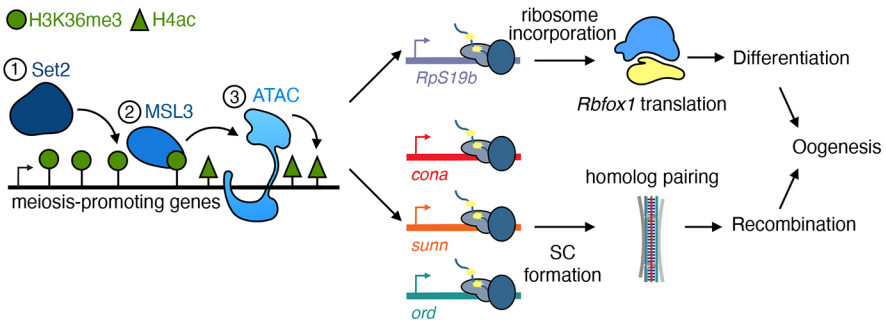

Fig. 7. Schematic of how Set2, Msl3 and the ATAC complex regulate oogenesis. Set2, Msl3 and the ATAC complex regulate transcription of *RpS19b* and SC components. RpS19b promotes translation of differentiation factor Rbfox1 to promote oogenesis.

Development (2022) 149, dev199625. doi:10.1242/dev.199625

transcriptional level by Set2, Msl3 and ATAC, components such as C(3)G and Crossover suppressor on 2 of Manheim [C(2)M] are not. This suggests that some synaptonemal complex members, such as C(2)M and C(3)G, might be regulated at the post-transcriptional level. Taken together, these data argue that the Set2-Msl3-ATAC complex coordinates the transcription of several crucial factors of the recombination machinery and the translation of a meiotic cell cycle regulator to promote proper oogenesis (Fig. 7).

MATERIALS AND METHODS

Fly lines

Flies were grown at 25-31°C and dissected between 1 and 5 days post-eclosion. The following RNAi stocks were used in this study (if more than one line is listed, then both were quantitated and the first is shown in the main figure): *Set2* RNAi [Bloomington Drosophila Stock Center (BDSC) #33706 (#1) and #42511 (#2)], *msl3* RNAi (BDSC #35272), *NC2β* RNAi [BDSC #57421 (#1) and VDRC #v3161 (#2)], *Ada2a* RNAi (BDSC #50905), *Atac1* RNAi [Vienna Drosophila Resource Center (VDRC) #v36092], *Atac2* RNAi (VDRC #v16047), *D12* RNAi (VDRC #v29954), *wds* RNAi (BDSC #60399), *NC2α* RNAi (BDSC #67277), *bam* RNAi (BDSC #58178), *hs-bam*/TM3 (BDSC #24637), *RpS19b* RNAi (VDRC #v22073 and #v102171) and *RpS19a* RNAi (BDSC #42774 and VDRC #v107188).

The following mutant and overexpression stocks were used in this study: $Set2^{1}$/FM7 (BDSC #77916), $msl3^{1}$/TM3 (BDSC #5872), $msl3^{KG}$/TM3 (BDSC #13165), $mls3^{MB}$/TM3 (BDSC #29244), $msl1^{y216}$/CyO (BDSC #5870), $msl1^{kmB}$/CyO (BDSC #25157), $msl2^{227}$/CyO (BDSC #5871), $msl2^{kmA}$/CyO (BDSC #25158), mle^{1}/SM1 (BDSC #4235), mle^{9}/CyO (BDSC #5873), $Hel89B^{08724}$/TM3 (BDSC #11732), *Hel89B Df*/TM6 (BDSC #7982), $Atac2^{e03046}$/CyO (BDSC #18111), $RpS19b^{EY00801}$ (BDSC #15043), $RpS19b^{CRISPR}$ (this study), *UAS-hRpS19-HA* (BDSC #66014) and *UAS-msl3-GFP* (this study).

The following tagged lines were used in this study: *msl3-GFP* (Kuroda Lab, Brigham and Women's Hospital, Boston, MA, USA), *RpS19a-3xHA* (this study), *RpS19b-GFP* (this study), and *ord-GFP* (Bickel Lab, Dartmouth College, Hanover, NH, USA).

The following tissue-specific drivers were used in this study: *UAS-Dcr2; nosGAL4* (BDSC #25751), *UAS-Dcr2;nosGAL4;bam-GFP* (Lehmann Lab, Whitehead Institute, MIT, Cambridge, MA, USA) and *If*/CyO*;nosGAL4* (Lehmann Lab). We used *UAS-Dcr2;nosGAL4* for all RNAi experiments, as this combination as it gave us the most consistent phenotype with the most germline in all genotypes indicated.

Dissection and immunostaining

Ovaries were dissected and stained as previously described (McCarthy et al., 2018). The following primary antibodies were used: mouse anti-1B1 (1:20; DSHB), rabbit anti-Vasa (1:1000; Rangan Lab, University at Albany, SUNY, USA), chicken anti-Vasa (1:1000; Upadhyay et al., 2016), rabbit anti-GFP (1:2000; Abcam, ab6556), guinea pig anti-Rbfox1 (1:1000; Tastan et al., 2010), mouse anti-C(3)G (1:1000; Hawley Lab, Stowers Institute, Kansas City, MO, USA), rabbit anti-H3K36me3 (1:500; Abcam, ab9050), rabbit anti-pMAD (1:150; Abcam, ab52903), mouse anti-BamC (1:200; DSHB, Supernatant), rabbit anti-Bru (1:500; Lehmann Lab), rabbit anti-Egl (1:1000; Lehmann Lab), rat anti-HA (1:500; Roche, 11 867 423 001) and rabbit anti-RpS19 (1:20; Proteintech, 15085-1-AP). Anti-RpS19 was pre-cleared at 1:20, the supernatant was then diluted at 1:2.5 for staining. The following secondary antibodies were used at a dilution of 1:500: Alexa 488 (Molecular Probes), and Cy3 and Cy5 (Jackson Labs).

Fluorescence imaging

The tissues were visualized and images were acquired using a Zeiss LSM-710 confocal microscope under 20×, 40× and 63× oil objectives.

Quantification of phenotypes

We quantified loss of germline by counting ovarioles that did not have Vasa-positive cells. For loss of stem cells, we quantified loss of spectrosome-containing cells. For cyst differentiation defect, we counted the number of germaria with cysts containing more than 16 cells and/or accumulation of 16-cell cysts close to the niche.

AU quantification of protein or *in situ*

To quantify antibody staining intensities for Rbfox1, H3K36me3, Bruno, GFP, HA and RpS19 or *in situ* probe fluorescence in germ cells, images for both control and experimental germaria were taken using the same confocal settings. *Z* stacks were obtained for all images. Similar planes in control and experimental germaria were chosen, the area of germ cells positive for the proteins or *in situs* of interest was outlined and analyzed using the 'analyze' tool in Fiji (ImageJ). The mean intensity and area of the specified region was obtained. An average of all the ratios (mean/area), for the proteins or *in situs* of interest, per image was calculated for both control and experimental. Germline intensities were normalized to somatic intensities or, if the protein or *in situ* of interest is germline enriched and not expressed in the soma, they were normalized to Vasa or background. The highest mean intensity between control and experimental(s) was used to normalize to a value of 1 arbitrary unit (AU) on the graph. A minimum of five germaria was used for quantitation.

Egg laying assays

Assays were conducted in cages with females under testing and wild-type control males. Cages were maintained at 25°C. All flies were 1 day post-eclosion upon setting up the experiment and analyses were performed on four consecutive days. The number of eggs laid were normalized to the total number of females.

RNA-seq library preparation and analysis

Ovaries from flies of various genotypes were dissected in 1×PBS. For enriching GSCs, we over overexpressed TKV in the germline, for CBs, we used *bam* mutant and for cysts we used *bam* mutant also carrying a *hsbam* transgene. Post heat-shock CBs converted to cysts. RNA was isolated using TRIzol (Invitrogen, 15596026), treated with DNase (TURBO DNA-free Kit, Life Technologies, AM1907) and then run on a 1% agarose gel to check the integrity of the RNA. To generate mRNA-enriched libraries, total RNA was treated with poly(A)tail selection beads (Bioo Scientific, NOVA-512991) and then following the manufacturer's instructions of the NEXTflex Rapid Directional RNA-seq Kit (Bioo Scientific, NOVA-5138-08), except that RNA was fragmented for 13 min. Single-end mRNA sequencing (75 base pair) was performed on biological duplicates from each genotype on an Illumina NextSeq500 by the Center for Functional Genomics (CFG).

After quality assessment, the sequenced reads were aligned to the *Drosophila melanogaster* genome (UCSCdm6) using HISAT2 (version 2.1.0) with the RefSeq-annotated transcripts as a guide (Kim et al., 2015). Raw counts were generated using featureCounts (version 1.6.0.4) (Liao et al., 2014). Differential gene expression was assayed by edgeR (version 3.16.5), using a false discovery rate (FDR) of 0.05, and genes with fourfold or higher differential expression were considered significant. The raw and unprocessed data for RNA-seq generated during this study have been deposited in GEO under accession number GSE143728.

In situ hybridization

Adult ovaries (five ovary pairs per sample per experiment) were dissected and fixed as previously described. The ovaries were washed with PT [1× phosphate-buffered saline (PBS) and 0.1% Triton-X 100) three times for 5 min each. Ovaries were permeabilized by washing once with increasing concentrations of methanol for 5 min each (30% methanol in PT, 50% methanol in PT and 70% methanol in PT) then incubating in methanol for 10 min. Ovaries were then post-fixed by washing once with decreasing concentrations of methanol for 5 min each (70% methanol in PT, 50% methanol in PT and 30% methanol in PT). Ovaries were then washed with PT three times for 5 min and then pre-hybridized in wash buffer for 10 min (10% deionized formamide and 10% 20× SSC in RNase-free water). Ovaries were incubated overnight in hybridization solution (10% dextran sulfate, 1 mg/ml yeast tRNA, 2 mM RNaseOUT, 0.02 mg/ml BSA, 5×SSC, 10% deionized formamide and RNase-free water) at 30°C. The hybridization solution was removed, and ovaries washed with wash buffer twice for 30 min at 30°C. Wash buffer was removed, and

Development (2022) 149, dev199625. doi:10.1242/dev.199625

ovaries were mounted using Vectashield with 4′,6′-diamidino-2-phenylindole (DAPI).

In situ probe design and generation

Templates were amplified with gene-specific primers (listed below) and then fluorescently labeled probes were generated by following the manufacturer's instructions (Thermo Fisher's FISH tag RNA kit, F32954): Rbfox1 F, 5′-CGTAGCGCCTTTTCCGGG-3′; Rbfox1 R, 5′-TAATACGACTCACTATAGGGCCACAGCCGCCACTTGAATA-3′; RpS19b F, 5′-TGCCTGGAGTCACAGTAAAGG-3′; RpS19b R, 5′-TAATACGACTCACTATAGGGTGTTGGCTATGCGATCCAAGT-3′; RpS19a F, 5′-ATGCCAGGCGTCACAGTGAA-3′; RpS19a R, 5′-TAATACGACTCACTATAGGGTTACTTGGAAATAACAATGGGCCC-3′.

Measurement of global protein synthesis

Protein synthesis was detected using a short-term ovary incorporation assay, Click-iT Plus OPP (Invitrogen, C10456). Ovaries were dissected in Schneider's *Drosophila* media (Thermo Fisher, 21720024) and then incubated in 50 µM OPP reagent for 30 min. Tissue was washed in 1× PBS and then fixed for 15 min in 1× PBS plus 5% methanol-free formaldehyde. Tissue was then permeabilized with 1% Triton X-100 in 1× PBST (1× PBS with 0.2% Tween 20) for 30 min, and samples were then washed in 1× PBS and incubated in Click-iT reaction cocktail following the manufacturer's instructions. Samples were washed with Click-iT reaction rinse buffer and then immunostained following previously described procedures.

Generating fly lines

CRISPR mutant

To generate the *RpS19b* mutants, guide RNAs were designed using https://flycrispr.org/target-finder/ and synthesized as 5-unphosphorylated oligonucleotides, annealed, phosphorylated and ligated into the BbsI sites of the pU6-BbsI-chiRNA vector using the primers listed below (Gratz et al., 2013). Homology arms were synthesized as a gene block (IDTDNA) and cloned into pHD-dsRed-attP (Gratz et al., 2015; Addgene plasmid #51019) using Gibson Assembly (gene blocks listed in the supplementary Materials and Methods). Guide RNAs and the donor vector were co-injected into *nos-Cas9* embryos (Rainbow Transgenics): RpS19b gRNA1 F, 5′-CTTCGCATGCCTGGAGTCACAGTAA-3′; RpS19b gRNA1 R, 5′-AAACTTACTGTGACTCCAGGCATGC-3′; RpS19b gRNA2 F, 5′-CTTCGTAGTGATAATCATGGAAAC-3′; RpS19b gRNA2 R, 5′-AAACGTTTCCATGATTATCACTAC-3′.

RpS19a-3xHA and RpS19b-GFP tagged lines

RpS19a3x-HA- (referred to as *RpS19a-HA* throughout the text) and *RpS19b-GFP*-tagged lines were made using a combination of *in vivo* bacterial recombineering and GatewayTM Technology as previously described (Shalaby et al., 2017).

UAS-msl3-GFP overexpression line

RNA was extracted from w^{1118} ovaries and made into cDNA using the SuperScript II-Strand Kit (Thermo Fisher, 18064014). *msl3* CDS was amplified, *att*B sites and tagged sequence were amplified into the PCR product using the primers listed below. PCR products were cloned into pDONR (Thermo Fisher, 11789-020) and swapped into pENTR (Thermo Fisher, 11791-020) using BP and LR reactions, respectively. The plasmid was sent for injection into w^{1118} flies (Genetic Services). PCR primers are as follows: msl3 CDS F, 5′-ATGACGGAGCTAAGGGACGAGAC-3′; msl3 CDS R, 5′-CTAAGCAGCAATCCCATCCAGGG-3′; attB F, 5′-GGGGACAAGTTTGTACAAAAAAGCAGGCTTCATGACGGAGCTAAGGGACGAGAC-3′; attB R, 5′-GGGGACCACTTTGTACAAGAAAGCTGGGTCCTAAGCGTAATCTGGCACATCGTATGGGTAAGCAGCAATCCCATCCAGGG-3′.

Polysome profiling and polysome-seq

Polysome profiling of ovaries from *bam* RNAi*;hs-bam* and *UAS-Dcr2; nosGAL4 >RpS19b* RNAi flies was adapted from Flora et al., (2018) and Fuchs et al. (2011). Two-hundred ovary pairs were dissected in Schneider's media and immediately flash frozen with liquid nitrogen. Ovaries were homogenized in lysis buffer, 20% of lysate was used as input for mRNA isolation and library preparation (as described above). Samples were loaded onto 10-50% CHX-supplemented sucrose gradients in 9/16×3.5 PA tubes (Beckman Coulter, 331372) and spun at 35,000 ***g*** in SW41 for 2.45-3 h at 4°C. Gradients were fractionated with a Density Gradient Fractionation System (Brandel, 621140007). RNA was extracted using acid phenol-chloroform and precipitated overnight. Pelleted RNA was resuspended in 20 µl water and libraries were prepared as described above.

Western blot

Fifty to 200 C-enriched *RpS19b-GFP* ovaries and 30 adult *RpS19b-GFP; RpS19a-HA* ovaries were dissected and prepared as described above, except sucrose solutions were supplemented with either 100 µg/µl CHX or 2 mM puromycin with 1 mg heparin prior to making gradients. Following fractionation, protein was extracted by ethanol precipitation and run on a TGX pre-cast gradient gel (BioRad, 456-1094). Blots were blocked with 5% milk in 1× PBST and incubated in primary antibody in 5% BSA in 1× PBST. Following 1× PBST washing, blots were incubated in secondary antibody in 5% milk in 1× PBST. Blots were washed with 1× PBST and then imaged with chemi-luminescence kit (BioRad, 170-5060). The following primary antibodies were used: rabbit anti-GFP (1:4000; Abcam, ab6556), rat anti-HA (1:3000; Roche, 11 867 423 001), rabbit anti-RpS25 (1:1000; abcam, ab40820) and rabbit anti-RpS19 (1:1000; Proteintech, 15085-1-AP). The following secondary antibodies were used: anti-rat HRP (1:10,000; Jackson Labs, 112-035-003) and anti-rabbit HRP (1:10,000; Jackson Labs, 111-035-144).

Statistical analysis

Relative fluorescence signals were compared between control and experimental groups using parametric tests (Student *t*-test or one-way ANOVA). Horizontal lines on scatter dot plots represent mean with 95% confidence interval and stars on stacked bar graphs represent statistical significance of corresponding color data set. Reported *P*-values correspond to unpaired and two-tailed tests. Analysis of percentage defect were compared between control and experimental groups using Fisher's exact test. All analyses were performed using Prism 8 software (GraphPad) and are reported in figure legends.

Materials and reagents for fly husbandry

Fly food was made using previously described procedures (Upadhyay et al., 2018).

Acknowledgements

We are grateful to Drs Marlow and Siekhaus for comments. We thank Drs Kuroda, Bach, Lehmann, Hawley, Bickel and Fuchs for reagents. We thank the Bloomington Drosophila Stock Center, the Vienna Drosophila Resource Center and the Transgenic RNAi Project (NIH/NIGMS R01-GM084947) for fly stocks.

Competing interests

The authors declare no competing or financial interests.

Author contributions

Conceptualization: P.R.; Methodology: A.M.; Validation: A.M.; Formal analysis: A.M., K.S., E.T.M.; Investigation: A.M.; Data curation: A.M., K.S., E.T.M., M.U., S.J., N.D.W., P.E.F., M.B.; Writing - original draft: A.M.; Writing - review & editing: A.M., P.R.; Visualization: M.U.; Supervision: P.E.F., M.B., P.R.; Project administration: P.R.; Funding acquisition: M.B., P.R.

Funding

This work is funded by the National Institutes of Health (2R01GM111770-06 and RO1GM135628 to P.M., R01GM125812 to M.B., and 1R15HD0964110, 1R01HD097331-01 and 1R01DC017149-01A1 to P.F.). Deposited in PMC for release after 12 months.

Data availability

The raw and unprocessed data for RNA-seq generated during this study have been deposited in GEO under accession number GSE143728.

Peer review history
The peer review history is available online at https://journals.biologists.com/dev/article-lookup/doi/10.1242/dev.199625

References

Ables, E. T. (2015). Drosophila oocytes as a model for understanding meiosis: an educational primer to accompany "corolla is a novel protein that contributes to the architecture of the synaptonemal complex of Drosophila. *Genetics* **199**, 17-23. doi:10.1534/genetics.114.167940

Allis, C. D. and Jenuwein, T. (2016). The molecular hallmarks of epigenetic control. *Nat. Rev. Genet.* **17**, 487. doi:10.1038/nrg.2016.59

Anderson, L. K., Royer, S. M., Page, S. L., McKim, K. S., Lai, A., Lilly, M. A. and Hawley, R. S. (2005). Juxtaposition of C(2)M and the transverse filament protein C(3)G within the central region of Drosophila synaptonemal complex. *Proc. Natl. Acad. Sci. U.S.A.* **102**, 4482-4487. doi:10.1073/pnas.0500172102

Bachiller, D. and Sánchez, L. (1989). Further analysis on the male-specific lethal mutations that affect dosage compensation in Drosophila melanogaster. *Roux's Arch. Dev. Biol.* **198**, 34-38. doi:10.1007/BF00376368

Balicky, E. M., Endres, M. W., Lai, C. and Bickel, S. E. (2002). Meiotic cohesion requires accumulation of ORD on chromosomes before condensation. *Mol. Biol. Cell* **13**, 3890-3900. doi:10.1091/mbc.e02-06-0332

Bannister, A. J. and Kouzarides, T. (2011). Regulation of chromatin by histone modifications. *Cell Res.* **21**, 381-395. doi:10.1038/cr.2011.22

Barr, J., Charania, S., Gilmutdinov, R., Yakovlev, K., Shidlovskii, Y. and Schedl, P. (2019). The CPEB translational regulator, Orb, functions together with Par proteins to polarize the Drosophila oocyte. *PLoS Genet.* **15**, e1008012. doi:10.1371/journal.pgen.1008012

Bashaw, G. J. and Baker, B. S. (1997). The regulation of the Drosophila msl-2 gene reveals a function for Sex-lethal in translational control. *Cell* **89**, 789-798. doi:10.1016/S0092-8674(00)80262-7

Bell, O., Conrad, T., Kind, J., Wirbelauer, C., Akhtar, A., Schubeler, D. and Schübeler, D. (2008). Transcription-coupled methylation of histone H3 at Lysine 36 regulates dosage compensation by enhancing recruitment of the MSL complex in Drosophila melanogaster. *Mol. Cell. Biol.* **28**, 3401-3409. doi:10.1128/MCB.00006-08

Belote, J. M. (1983). Male-specific lethal mutations of drosophila melanogaster. II. Parameters of gene action during male development. *Genetics* **105**, 881-896. doi:10.1093/genetics/105.4.881

Bone, J. R., Lavender, J., Richman, R., Palmer, M. J., Turner, B. M. and Kuroda, M. I. (1994). Acetylated histone H4 on the male X chromosome is associated with dosage compensation in Drosophila. *Genes Dev.* **8**, 96-104. doi:10.1101/gad.8.1.96

Carpenter, A. T. (1994). Egalitarian and the choice of cell fates in Drosophila melanogaster oogenesis. *Ciba Found. Symp.* **182**, 223-246.

Carpenter, A. T. and Sandler, L. (1974). On recombination-defective meiotic mutants in Drosophila melanogaster. *Genetics* **76**, 453-475. doi:10.1093/genetics/76.3.453

Carreira-Rosario, A., Bhargava, V., Hillebrand, J., Kollipara, R. K., Ramaswami, M. and Buszczak, M. (2016). Repression of pumilio protein expression by Rbfox1 promotes germ cell differentiation. *Dev. Cell* **36**, 562-571. doi:10.1016/j.devcel.2016.02.010

Chen, D. and McKearin, D. (2003a). Dpp signaling silences bam transcription directly to establish asymmetric divisions of germline stem cells. *Curr. Biol.* **13**, 1786-1791. doi:10.1016/j.cub.2003.09.033

Chen, D. and McKearin, D. M. (2003b). A discrete transcriptional silencer in the bam gene determines asymmetric division of the Drosophila germline stem cell. *Development (Cambridge, England)* **130**, 1159-1170. doi:10.1242/dev.00325

Christerson, L. B. and McKearin, D. M. (1994). orb Is required for anteroposterior and dorsoventral patterning during Drosophila oogenesis. *Genes Dev.* **8**, 614-628. doi:10.1101/gad.8.5.614

Cinalli, R. M., Rangan, P. and Lehmann, R. (2008). Germ cells are forever. *Cell* **132**, 559-562. doi:10.1016/j.cell.2008.02.003

Collins, K. A., Unruh, J. R., Slaughter, B. D., Yu, Z., Lake, C. M., Nielsen, R. J., Box, K. S., Miller, D. E., Blumenstiel, J. P., Perera, A. G. et al. (2014). Corolla is a novel protein that contributes to the architecture of the synaptonemal complex of Drosophila. *Genetics* **198**, 219-228. doi:10.1534/genetics.114.165290

Conrad, T., Cavalli, F. M. G., Holz, H., Hallacli, E., Kind, J., Ilik, I., Vaquerizas, J. M., Luscombe, N. M. and Akhtar, A. (2012a). The MOF chromobarrel domain controls genome-wide H4K16 acetylation and spreading of the MSL complex. *Dev. Cell* **22**, 610-624. doi:10.1016/j.devcel.2011.12.016

Conrad, T., Cavalli, F. M. G., Vaquerizas, J. M., Luscombe, N. M. and Akhtar, A. (2012b). Drosophila dosage compensation involves enhanced pol II recruitment to male X-linked promoters. *Science* **337**, 742-746. doi:10.1126/science.1221428

Dong, X. and Weng, Z. (2013). The correlation between histone modifications and gene expression. *Epigenomics* **5**, 113-116. doi:10.2217/epi.13.13

Eichhorn, S. W., Subtelny, A. O., Kronja, I., Kwasnieski, J. C., Orr-Weaver, T. L. and Bartel, D. P. (2016). mRNA poly(A)-tail changes specified by deadenylation broadly reshape translation in Drosophila oocytes and early embryos. *eLife* **5**, e16955. doi:10.7554/eLife.16955

El-Brolosy, M. A., Kontarakis, Z., Rossi, A., Kuenne, C., Günther, S., Fukuda, N., Kikhi, K., Boezio, G. L. M., Takacs, C. M., Lai, S.-L. et al. (2019). Genetic compensation triggered by mutant mRNA degradation. *Nature* **568**, 193-197. doi:10.1038/s41586-019-1064-z

Eliazer, S. and Buszczak, M. (2011). Finding a niche: studies from the Drosophila ovary. *Stem Cell Res. Ther.* **2**, 45. doi:10.1186/scrt86

Erickson, J. W. (2016). Primary sex determination in Drosophila melanogaster does not rely on the male-specific lethal complex. *Genetics* **202**, 541-549. doi:10.1534/genetics.115.182931

Flora, P., McCarthy, A., Upadhyay, M. and Rangan, P. (2017). Role of chromatin modifications in Drosophila germline stem cell differentiation. *Results Probl. Cell Differ.* **59**, 1-30. doi:10.1007/978-3-319-44820-6_1

Flora, P., Wong-Deyrup, S. W., Martin, E., Palumbo, R., Nasrallah, M., Oligney, A., Blatt, P., Patel, D., Fuchs, G. and Rangan, P. (2018). Sequential regulation of maternal mRNAs through a conserved cis-acting element in their 3 UTRs. *Cell Rep* **25**, 3828-3843.e9. doi:10.1016/j.celrep.2018.12.007

Fuchs, G., Diges, C., Kohlstaedt, L. A., Wehner, K. A. and Sarnow, P. (2011). Proteomic analysis of ribosomes: translational control of mRNA populations by glycogen synthase GYS1. *J. Mol. Biol.* **410**, 118-130. doi:10.1016/j.jmb.2011.04.064

Gladstein, N., McKeon, M. N. and Horabin, J. I. (2010). Requirement of male-specific dosage compensation in Drosophila females-implications of early X chromosome gene expression. *PLoS Genet.* **6**, e1001041. doi:10.1371/journal.pgen.1001041

Gratz, S. J., Cummings, A. M., Nguyen, J. N., Hamm, D. C., Donohue, L. K., Harrison, M. M., Wildonger, J. and O'Connor-Giles, K. M. (2013). Genome engineering of Drosophila with the CRISPR RNA-Guided Cas9 nuclease. *Genetics* **194**, 1029-1035. doi:10.1534/genetics.113.152710

Gratz, S. J., Rubinstein, C. D., Harrison, M. M., Wildonger, J. and O'Connor-Giles, K. M. (2015). CRISPR-Cas9 genome editing in Drosophila. *Curr. Protoc. Mol. Biol.* **111**, 31.2.1-31.2.20. doi:10.1002/0471142727.mb3102s111

Gu, W., Wei, X., Pannuti, A. and Lucchesi, J. C. (2000). Targeting the chromatin-remodeling MSL complex of Drosophila to its sites of action on the X chromosome requires both acetyl transferase and ATPase activities. *EMBO J.* **19**, 5202-5211. doi:10.1093/emboj/19.19.5202

Handel, M. A. and Schimenti, J. C. (2010). Genetics of mammalian meiosis: Regulation, dynamics and impact on fertility. *Nat. Rev. Genet.* **11**, 124-136. doi:10.1038/nrg2723

Hilfiker, A., Hilfiker-Kleiner, D., Pannuti, A. and Lucchesi, J. C. (1997). . mof, a putative acetyl transferase gene related to the Tip60 and MOZ human genes and to the SAS genes of yeast, is required for dosage compensation in Drosophila. *EMBO J.* **16**, 2054-2060. doi:10.1093/emboj/16.8.2054

Hua, B. L., Li, S. and Orr-Weaver, T. L. (2014). The role of transcription in the activation of a Drosophila amplification origin. *G3 (Bethesda, Md.)* **4**, 2403-2408. doi:10.1534/g3.114.014050

Hughes, S. E., Miller, D. E., Miller, A. L. and Hawley, R. S. (2018). Female Meiosis: Synapsis, Recombination, and Segregation in Drosophila melanogaster. *Genetics* **208**, 875-908. doi:10.1534/genetics.117.300081

Huynh, J. R. and St Johnston, D. (2000). The role of BicD, Egl, Orb and the microtubules in the restriction of meiosis to the Drosophila oocyte. *Development (Cambridge. England)* **127**, 2785-2794.

Kai, T. and Spradling, A. (2003). An empty Drosophila stem cell niche reactivates the proliferation of ectopic cells. *Proc. Natl. Acad. Sci. U.S.A.* **100**, 4633-4638. doi:10.1073/pnas.0830856100

Kelley, R. L., Wang, J., Bell, L. and Kuroda, M. I. (1997). Sex lethal controls dosage compensation in Drosophila by a non-splicing mechanism. *Nature* **387**, 195-199. doi:10.1038/387195a0

Keogh, M.-C. C., Kurdistani, S. K., Morris, S. A., Ahn, S. H., Podolny, V., Collins, S. R., Schuldiner, M., Chin, K., Punna, T., Thompson, N. J. et al. (2005). Cotranscriptional set2 methylation of histone H3 lysine 36 recruits a repressive Rpd3 complex. *Cell* **123**, 593-605. doi:10.1016/j.cell.2005.10.025

Kim, D., Blus, B. J., Chandra, V., Huang, P., Rastinejad, F. and Khorasanizadeh, S. (2010). Corecognition of DNA and a methylated histone tail by the MSL3 chromodomain. *Nat. Struct. Mol. Biol.* **17**, 1027-1029. doi:10.1038/nsmb.1856

Kim, D., Langmead, B. and Salzberg, S. L. (2015). HISAT: a fast spliced aligner with low memory requirements. *Nat. Methods* **12**, 357-360. doi:10.1038/nmeth.3317

Kimble, J. (2011). Molecular regulation of the mitosis/meiosis decision in multicellular organisms. *Cold Spring Harbor Perspect. Biol.* **3**, a002683. doi:10.1101/cshperspect.a002683

Larschan, E., Alekseyenko, A. A., Gortchakov, A. A., Peng, S., Li, B., Yang, P., Workman, J. L., Park, P. J. and Kuroda, M. I. (2007). MSL complex is attracted to genes marked by H3K36 trimethylation using a sequence-independent mechanism. *Mol. Cell* **28**, 121-133. doi:10.1016/j.molcel.2007.08.011

Lehmann, R. (2012). Germline stem cells: origin and destiny. *Cell Stem Cell* **10**, 729-739. doi:10.1016/j.stem.2012.05.016

Lesch, B. J. and Page, D. C. (2012). Genetics of germ cell development. *Nat. Rev. Genet.* **13**, 781-794. doi:10.1038/nrg3294
Liao, Y., Smyth, G. K. and Shi, W. (2014). featureCounts: an efficient general purpose program for assigning sequence reads to genomic features. *Bioinformatics (Oxford, England)* **30**, 923-930. doi:10.1093/bioinformatics/btt656
Lucchesi, J. C. and Kuroda, M. I. (2015). Dosage compensation in Drosophila. *Cold Spring Harbor Perspect. Biol.* **7**, a019398. doi:10.1101/cshperspect.a019398
Mach, J. M. and Lehmann, R. (1997). An Egalitarian-BicaudalD complex is essential for oocyte specification and axis determination in Drosophila. *Genes Dev.* **11**, 423-435. doi:10.1101/gad.11.4.423
Mathieu, J. and Huynh, J. R. (2017). Monitoring complete and incomplete abscission in the germ line stem cell lineage of Drosophila ovaries. *Methods Cell Biol.* **137**, 105-118. doi:10.1016/bs.mcb.2016.03.033
McCarthy, A., Deiulio, A., Martin, E. T., Upadhyay, M. and Rangan, P. (2018). Tip60 complex promotes expression of a differentiation factor to regulate germline differentiation in female Drosophila. *Mol. Biol. Cell* **29**, 2933-2945. doi:10.1091/mbc.E18-06-0385
McKearin, D. and Ohlstein, B. (1995). A role for the Drosophila bag-of-marbles protein in the differentiation of cystoblasts from germline stem cells. Development (Cambridge. *England* **121**, 2937-2947.
McKearin, D. M. and Spradling, A. C. (1990). . bag-of-marbles: a Drosophila gene required to initiate both male and female gametogenesis. *Genes Dev.* **4**, 2242-2251. doi:10.1101/gad.4.12b.2242
Meller, V. H., Wu, K. H., Roman, G., Kuroda, M. I. and Davis, R. L. (1997). roX1 RNA paints the X chromosome of male Drosophila and is regulated by the dosage compensation system. *Cell* **88**, 445-457. doi:10.1016/S0092-8674(00)81885-1
Morris, L. X. and Spradling, A. C. (2011). Long-term live imaging provides new insight into stem cell regulation and germline-soma coordination in the Drosophila ovary. *Development (Cambridge. England)* **138**, 2207-2215.
Morrison, S. J. and Spradling, A. C. (2008). Stem cells and niches: mechanisms that promote stem cell maintenance throughout life. *Cell* **132**, 598-611. doi:10.1016/j.cell.2008.01.038
Mukai, M., Hira, S., Nakamura, K., Nakamura, S., Kimura, H., Sato, M. and Kobayashi, S. (2015). H3K36 Trimethylation-mediated epigenetic regulation is activated by bam and promotes germ cell differentiation during early oogenesis in Drosophila. *Biology open* **4**, 119-124. doi:10.1242/bio.201410850
Navarro, C., Lehmann, R. and Morris, J. (2001). Oogenesis: Setting one sister above the rest. *Curr. Biol.* **11**, R162-R165. doi:10.1016/S0960-9822(01)00083-5
Navarro-Costa, P., McCarthy, A., Prudêncio, P., Greer, C., Guilgur, L. G., Becker, J. D., Secombe, J., Rangan, P. and Martinho, R. G. (2016). Early programming of the oocyte epigenome temporally controls late prophase i transcription and chromatin remodelling. *Nat. Commun.* **7**, 12331. doi:10.1038/ncomms12331
Ohlstein, B. and McKearin, D. (1997). Ectopic expression of the Drosophila Bam protein eliminates oogenic germline stem cells. *Development (Cambridge, England)* **124**, 3651-3662. doi:10.1242/dev.124.18.3651
Page, S. L. and Hawley, R. S. (2001). . c(3)G encodes a Drosophila synaptonemal complex protein. *Genes Dev.* **15**, 3130-3143. doi:10.1101/gad.935001
Parisi, M. J., Deng, W., Wang, Z. and Lin, H. (2001). The arrest gene is required for germline cyst formation during Drosophila oogenesis. *Genesis* **29**, 196-209. doi:10.1002/gene.1024
Parisi, M., Nuttall, R., Edwards, P., Minor, J., Naiman, D., Lü, J., Doctolero, M., Vainer, M., Chan, C., Malley, J. et al. (2004). A survey of ovary-, testis-, and soma-biased gene expression in Drosophila melanogaster adults. *Genome Biol.* **5**, R40. doi:10.1186/gb-2004-5-6-r40
Sanchez, C. G., Teixeira, F. K., Czech, B., Preall, J. B., Zamparini, A. L., Seifert, J. R. K., Malone, C. D., Hannon, G. J. and Lehmann, R. (2016). Regulation of ribosome biogenesis and protein synthesis controls germline stem cell differentiation. *Cell Stem Cell* **18**, 276-290. doi:10.1016/j.stem.2015.11.004
Shalaby, N. A., Sayed, R., Zhang, Q., Scoggin, S., Eliazer, S., Rothenfluh, A. and Buszczak, M. (2017). Systematic discovery of genetic modulation by Jumonji histone demethylases in Drosophila. *Sci. Rep.* **7**, 5240. doi:10.1038/s41598-017-05004-w
Soh, Y. Q. S., Junker, J. P., Gill, M. E., Mueller, J. L., van Oudenaarden, A. and Page, D. C. (2015). A gene regulatory program for meiotic prophase in the fetal ovary. *PLoS Genet.* **11**, e1005531. doi:10.1371/journal.pgen.1005531
Spedale, G., Timmers, H. T. M. and Pijnappel, W. W. M. P. (2012). ATAC-king the complexity of SAGA during evolution. *Genes Dev.* **26**, 527-541. doi:10.1101/gad.184705.111
Spradling, A. C., de Cuevas, M., Drummond-Barbosa, D., Keyes, L., Lilly, M., Pepling, M. and Xie, T. (1997). The Drosophila germarium: stem cells, germ line cysts, and oocytes. *Cold Spring Harbor Symp. Quant. Biol.* **62**, 25-34. doi:10.1101/SQB.1997.062.01.006
Spradling, A., Drummond-Barbosa, D. and Kai, T. (2001). Stem cells find their niche. *Nature* **414**, 98-104. doi:10.1038/35102160
Spradling, A. C., Nystul, T., Lighthouse, D., Morris, L., Fox, D., Cox, R., Tootle, T., Frederick, R. and Skora, A. (2008). Stem cells and their niches: integrated units that maintain Drosophila tissues. *Cold Spring Harbor Symp. Quant. Biol.* **73**, 49-57. doi:10.1101/sqb.2008.73.023
Spradling, A., Fuller, M. T., Braun, R. E. and Yoshida, S. (2011). Germline stem cells. *Cold Spring Harbor Perspect. Biol.* **3**, a002642. doi:10.1101/cshperspect.a002642
Stabell, M., Larsson, J., Aalen, R. B. and Lambertsson, A. (2007). Drosophila dSet2 functions in H3-K36 methylation and is required for development. *Biochem. Biophys. Res. Commun.* **359**, 784-789. doi:10.1016/j.bbrc.2007.05.189
Strukov, Y. G., Sural, T. H., Kuroda, M. I. and Sedat, J. W. (2011). Evidence of activity-specific, radial organization of mitotic chromosomes in Drosophila. *PLoS Biol.* **9**, e1000574. doi:10.1371/journal.pbio.1000574
Suganuma, T., Gutiérrez, J. L., Li, B., Florens, L., Swanson, S. K., Washburn, M. P., Abmayr, S. M. and Workman, J. L. (2008). ATAC is a double histone acetyltransferase complex that stimulates nucleosome sliding. *Nat. Struct. Mol. Biol.* **15**, 364-372. doi:10.1038/nsmb.1397
Sugimura, I. and Lilly, M. A. (2006). Bruno inhibits the expression of mitotic cyclins during the prophase I meiotic arrest of Drosophila oocytes. *Dev. Cell* **10**, 127-135. doi:10.1016/j.devcel.2005.10.018
Sun, J., Wei, H.-M., Xu, J., Chang, J.-F., Yang, Z., Ren, X., Lv, W.-W., Liu, L.-P., Pan, L.-X., Wang, X. et al. (2015). Histone H1-mediated epigenetic regulation controls germline stem cell self-renewal by modulating H4K16 acetylation. *Nat. Commun.* **6**, 8856. doi:10.1038/ncomms9856
Sural, T. H., Peng, S., Li, B., Workman, J. L., Park, P. J. and Kuroda, M. I. (2008). The MSL3 chromodomain directs a key targeting step for dosage compensation of the Drosophila melanogaster X chromosome. *Nat. Struct. Mol. Biol.* **15**, 1318-1325. doi:10.1038/nsmb.1520
Tastan, O. Y., Maines, J. Z., Li, Y., McKearin, D. M. and Buszczak, M. (2010). Drosophila ataxin 2-binding protein 1 marks an intermediate step in the molecular differentiation of female germline cysts. *Development (Cambridge, England)* **137**, 3167-3176. doi:10.1242/dev.050575
The Modencode Consortium, Roy, S., Ernst, J., Kharchenko, P. V., Kheradpour, P., Negre, N., Eaton, M. L., Landolin, J. M., Bristow, C. A., Ma, L. et al. (2010). Identification of functional elements and regulatory circuits by Drosophila modENCODE. *Science* **330**, 1787-1797.
Theurkauf, W. E., Alberts, B. M., Jan, Y. N. and Jongens, T. A. (1993). A central role for microtubules in the differentiation of Drosophila oocytes. *Development (Cambridge. England)* **118**, 1169-1180.
Uchida, S., Uenoyama, T. and Oishi, K. (1981). Studies on the sex-specific lethals of Drosophila melanogaster. III. A third chromosome male-specific lethal mutant. *Jap. J. Genet.* **56**, 523-527. doi:10.1266/jjg.56.523
Upadhyay, M., Kuna, M., Tudor, S., Martino Cortez, Y. and Rangan, P. (2018). A switch in the mode of Wnt signaling orchestrates the formation of germline stem cell differentiation niche in Drosophila. *PLoS Genet.* **14**, e1007154. doi:10.1371/journal.pgen.1007154
Upadhyay, M., Martino Cortez, Y., Wong-Deyrup, S., Tavares, L., Schowalter, S., Flora, P., Hill, C., Nasrallah, M. A., Chittur, S. and Rangan, P. (2016). Transposon dysregulation modulates dWnt4 signaling to control germline stem cell differentiation in Drosophila. *PLoS Genet.* **12**, e1005918. doi:10.1371/journal.pgen.1005918
Von Stetina, J. R. and Orr-Weaver, T. L. (2011). Developmental control of oocyte maturation and egg activation in metazoan models. *Cold Spring Harbor Perspect. Biol.* **3**, a005553. doi:10.1101/cshperspect.a005553
Wang, Z. and Lin, H. (2007). Sex-lethal is a target of Bruno-mediated translational repression in promoting the differentiation of stem cell progeny during Drosophila oogenesis. *Dev. Biol.* **302**, 160-168. doi:10.1016/j.ydbio.2006.09.016
Xie, T. (2013). Control of germline stem cell self-renewal and differentiation in the Drosophila ovary: concerted actions of niche signals and intrinsic factors. Wiley interdisciplinary reviews. *Dev. Biol.* **2**, 261-273.
Xie, T. and Spradling, A. C. (1998). decapentaplegic is essential for the maintenance and division of germline stem cells in the Drosophila ovary. *Cell* **94**, 251-260. doi:10.1016/S0092-8674(00)81424-5
Zhang, Q., Shalaby, N. A. and Buszczak, M. (2014). Changes in rRNA transcription influence proliferation and cell fate within a stem cell lineage. *Science (New York, N.Y.)* **343**, 298-301. doi:10.1126/science.1246384